The Star Formation Newsletter

A community newsletter on Star and Planet Formation research

No. 357 — 30 September 2022
Editor: João Alves
www.starformation.news

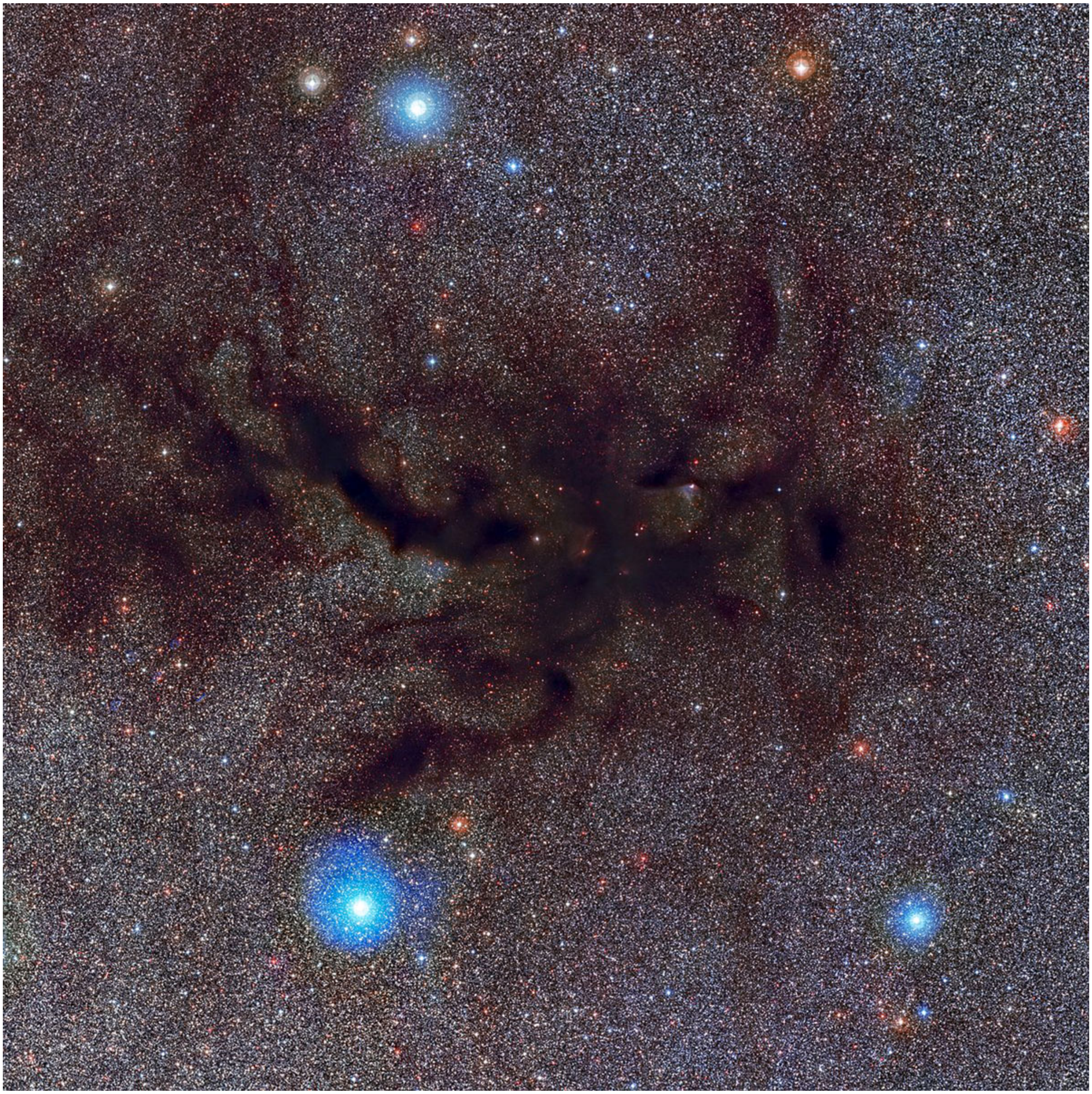

Links to sections

Interviews | Reviews | Perspective | Favorite objects | Archive
Meetings | Jobs | New PhDs | Announcements | Books

Cover image caption

Barnard 59, or B59, is the northern tip of the nearby Pipe Nebula dark cloud (the Pipe's mouthpiece). Barnard 59 contains about 20 YSOs, most deeply embedded towards this cloud's center, and it is one of the closest embedded clusters of YSOs to Earth, less well studied than the better-known L1688 in Ophiuchus (rho Oph core). The image was captured by the Wide Field Imager on the MPG/ESO 2.2-metre telescope at ESO's La Silla Observatory.

Credit: ESO, MPG/ESO 2.2-m telescope

Note from the Editor

The Star Formation Newsletter is now on the web at **www.starformation.news**. This PDF file contains the monthly Abstracts and links to the different Newsletter sections. Red text in this PDF is a url link. Submitting an abstract to the SFN is as simple as entering the arXiv ID (e.g., 2006.10139) in a web form on the SFN web site. **Do not remove the LaTeX formatting when submitting to the arXiv**. If you do, your abstract will not look great either at the arXiv or the SFN.

Abstracts

1. Ices in planet-forming disks: Self-consistent ice opacities in disk models

Aditya M. Arabhavi, Peter Woitke, Stephanie M. Cazaux, Inga Kamp, Christian Rab, Wing-Fai Thi ★ In cold and shielded environments, molecules freeze out on dust grain surfaces to form ices such as H2O, CO, CO2, CH4, CH3OH, and NH3. In protoplanetary disks, the exact radial and vertical ice extension depend on disk mass, geometry, and stellar UV irradiation. The goal of this work is to present a computationally efficient method to compute ice and bare-grain opacities in protoplanetary disk models consistently with the chemistry and to investigate the effect of ice opacities on the physico-chemical state and optical appearance of the disk. A matrix of Mie efficiencies is pre-calculated for different ice species and thicknesses, from which the position dependent opacities of icy grains are then interpolated. This is implemented in the PRODIMO code by a self-consistent solution of ice opacities and the local composition of ices, which are obtained from our chemical network. Locally, the opacity can change significantly, for example, an increase by a factor of more than 200 in the midplane, especially at UV and optical wavelengths, due to ice formation. This is mainly due to changes in the size distribution of dust grains resulting from ice formation. However, since the opacity only changes in the optically thick regions of the disk, the thermal disk structure does not change significantly. For the same reason, the spectral energy distributions computed with our disk models with ice opacities generally show only faint ice emission features at far-IR wavelengths. The ice absorption features are only seen in the edgeon orientation. The assumption made on how the ice is distributed across the grain size distribution influences the far-IR and millimeter slope of the SED. The ice features and their strengths are influenced by the ice power law and the type of chemistry. Our models predict stronger ice features for observations that can spatially resolve the disk, particularly in absorption.

2. Tracing the contraction of the pre-stellar core L1544 with $HC^{17}O^+$ $J = 1$-0 emission

J. Ferrer Asensio, S. Spezzano, P. Caselli, F. O. Alves, O. Sipilä, E. Redaelli, L. Bizzocchi, F. Lique, A. Mullins ★ Spectral line profiles of several molecules observed towards the pre-stellar core L1544 appear double-peaked. For abundant molecular species this line morphology has been linked to self-absorption. However, the physical process behind the double-peaked morphology for less abundant species is still under debate. In order to understand the cause behind the double-peaked spectra of optically thin transitions and their link to the physical structure of pre-stellar cores, we present high-sensitivity and high-spectral resolution $HC^{17}O^+$ J =1-0 observations towards the dust peak in L1544. We observed the $HC^{17}O^+$ (1-0) spectrum with the Institut de Radioastronomie Millimétrique (IRAM) 30m telescope. By using new state-of-the-art collisional rate coefficients, a physical model for the core and the fractional abundance profile of $HC^{17}O^+$, the hyperfine structure of this molecular ion is modelled for the first time with the radiative transfer code LOC applied to the predicted chemical structure of a contracting pre-stellar core. We applied the same analysis to the chemically related $C^{17}O$ molecule. The observed $HC^{17}O^+$(1-0) and $C^{17}O$(1-0) lines have been successfully reproduced with a non-local thermal equilibrium (LTE) radiative transfer model applied to chemical model predictions for a contracting pre-stellar core. An upscaled velocity profile (by 30observations. The double peaks observed in the $HC^{17}O^+$(1-0) hyperfine components are due to the contraction motions at densities close to the critical density of the transition ($\sim 10^5$ cm^{-3}) and to the fact that the HCO^+ fractional abundance decreases toward the centre.

3. Volatile-rich comets ejected early on during Solar System formation

S. E. Anderson, J. -M. Petit, B. Noyelles, O. Mousis, P. Rousselot ★ Comet C/2016 R2 PanSTARRS (hereafter C/2016 R2) presents an unusually high N2/CO abundance ratio, as well as a heavy depletion in H2O, making it the only known comet of its kind. Understanding its dynamical history is therefore of essential importance as it would allow us to gain a clearer understanding of the evolution of planetesimal formation in our Solar System. Two studies have independently estimated the possible origin of this comet from building blocks formed in a peculiar region of the protoplanetary disk, near the ice line of CO and N2. We intend to investigate the fates of objects formed from the building blocks in these regions. We hope to find a possible explanation for the lack of C/2016 R2-like comets in our Solar System. Using a numerical simulation of the early stages of Solar System formation, we track the dynamics of these objects in the Jumping Neptune scenario based on five different initial conditions for the protosolar disk. We integrate the positions of 250 000 planetesimals over time in order to analyze the evolution of their orbits and create a statistical profile of their expected permanent orbit. Results. We find that objects formed in the region of the CO- and N2- ice lines are highly likely to be sent towards the Oort Cloud or possibly ejected from the Solar System altogether on a relatively short timescale. In all our simulations, over 90in this region evolved into a hyperbolic trajectory, and between 1were potentially captured by the Oort Cloud. The handful of comets that remained were either on long-period, highly eccentric orbits like C/2016 R2, or absorbed into the Edgeworth-Kuiper belt. Comets formed <15 au were predominantly ejected early in the formation timeline. As this is the formation zone likely to produce comets of this composition, this process could explain the lack of similar comets observed in the Solar System

4. The Star Formation-Gas Density Relation in Four Galactic GMCs: Effects of Stellar Feedback

John H. Bieging, Shuo Kong ★ We present maps of 4 galactic giant molecular clouds (GMCs) in the J=2-1 emission of both CO and ^{13}CO. We use an LTE analysis to derive maps of the CO excitation temperature and column density and the distribution of total molecular gas column density, Σ_{gas}. The depletion of CO by freeze-out onto cold dust grains is accounted for by an approximation to the results of Lewis et al. (2021) which were derived from far-IR observations with *Herschel*. The surface density of young stellar objects (YSOs) is obtained from published catalogs. The mean YSO surface density exhibits a power-law dependence on Σ_{gas}, with exponents in the range 0.9 to 1.9. Gas column density probability distribution functions (PDFs) show power-law tails extending to high column densities. The distributions of sonic Mach number, M_S are sharply peaked at $M_S \sim 5-8$ for 3 GMCs; a fourth has a broad distribution up to $M_S = 30$, possibly a result of feedback effects from multiple OB stars. An analysis following the methodology of Pokhrel et al. (2021) finds that our sample of GMCs shows power-law relations that are somewhat shallower than found by Pokhrel et al. (2021) for the star formation rate vs. $<\Sigma_{gas}>$ and vs. $<\Sigma_{gas}>/t_{ff}$ in a different sample of clouds. We discuss possible differences in the two samples of star-forming clouds and the effects of stellar feedback on the relation between gas density and star formation rate.

5. Possible Explosive Dispersal Outflow in IRAS 16076-5134 revealed with ALMA

Estrella Guzmán Ccolque, Manuel Fernández-López, Luis A. Zapata, Tapas Baug ★ We present 0.9 mm continuum and CO (3-2) line emission observations retrieved from the Atacama Large Millimeter/submillimeter Array (ALMA) archive toward the high-mass star formation region IRAS 16076-5134. We identify fourteen dense cores with masses between 0.3 to 22 $M_\odot$. We find an ensemble of filament-like CO (3-2) ejections from -62 to +83 km s^{-1} that appear to arise radially from a common central position, close to the dense core MM8. The ensemble of filaments, has a quasi-isotropic distribution in the plane of the sky. The radial velocity of several filaments follow a linear velocity gradient, incresing from a common origin. Considering the whole ensemble of filaments, we estimate its total mass to be 138 and 216 $M_\odot$ from its CO emission, for 70 K and 140 K respectively. Also, assuming a constant velocity expansion of the filaments (of 83 km s^{-1}) we estimate the dynamical age of the outflowing material (3500 years), its momentum (10^4 $M_\odot$ km s^{-1}) and its kinetic energy (10^{48-49} erg). The morphology and kinematics presented by the filaments suggest the presence of a dispersal outflow with explosive characteristics in IRAS 16076-5134. In addition, we make a raw estimate of the lower limit of the frequency rate of the explosive dispersal outflows in the Galaxy (one every 110 years) considering constant star formation rate and efficiency with respect to the galactocentric radius of the Galaxy. This may imply a comparable rate of dispersal outflows and supernovae (approximately one every 50 years), which may be important for the energy budget of the Interstellar Medium and the link between dispersal outflows and high-mass star formation.

6. Turbulence and Accretion: a High-resolution Study of the B5 Filaments

Michael Chun-Yuan Chen, James Di Francesco, Jaime E. Pineda, Stella S. Offner, Rachel K. Friesen ★ High-resolution observations of the Perseus B5 "core" have previously revealed that this subsonic region actually consists of several filaments that are likely in the process of forming a quadruple stellar system. Since subsonic filaments are thought to be produced at the ~ 0.1 pc sonic scale by turbulent compression, a detailed kinematic study is crucial to test such a scenario in the context of core and star formation. Here we present a detailed kinematic follow-up study of the B5 filaments at a 0.009 pc resolution using the VLA and GBT combined observations fitted with multi-component spectral models. Using precisely identified filament spines, we find a remarkable resemblance between the averaged width profiles of each filament and Plummer-like functions, with filaments possessing FWHM widths of ~ 0.03 pc. The velocity dispersion profiles of the filaments also show decreasing trends towards the filament spines. Moreover, the velocity gradient field in B5 appears to be locally well ordered (~ 0.04 pc) but globally complex, with kinematic behaviors suggestive of inhomogeneous turbulent accretion onto filaments and longitudinal flows towards a local overdensity along one of the filaments.

7. Rethinking the role of the giant planet instability in terrestrial planet formation models

Matthew S. Clement, Rogerio Deienno, Andre Izidoro ★ Advances in computing power and numerical methodologies over the past several decades sparked a prolific output of dynamical investigations of the late stages of terrestrial planet formation. Among other peculiar inner solar system qualities, the ability of simulations to reproduce the small mass of Mars within the planets' geochemically inferred accretion timescale of <10 Myr after the appearance of calcium aluminum-rich inclusions (CAIs) is arguably considered the gold standard for judging evolutionary hypotheses. At present, a number of independent models are capable of consistently generating Mars-like planets and simultaneously satisfying various important observational and geochemical constraints. However, all models must still account for the effects of the epoch of giant planet migration and orbital instability; an event which dynamical and cosmochemical constraints indicate occurred within the first 100 Myr after nebular gas dispersal. If the instability occurred in the first few Myr of this window, the disturbance might have affected the bulk of Mars' growth. In this manuscript, we turn our attention to a scenario where the instability took place after t=50 Myr. Specifically, we simulate the instability's effects on three nearly-assembled terrestrial systems that were generated via previous embryo accretion models and contain three large proto-planets with orbits interior to a collection of Mars-mass embryos and debris. While the instability consistently triggers a Moon-forming impact and efficiently removes excessive material from the Mars-region in our models, we find that our final systems are too dynamically excited and devoid of Mars and Mercury analogs. Thus, we conclude that, while possible, our scenario is far more improbable than one where the instability either occurred earlier, or at a time where Earth and Venus' orbits were far less dynamically excited.

8. Turbulence in outer protoplanetary disks: MRI or VSI?

Can Cui, Xue-Ning Bai ★ The outer protoplanetary disks (PPDs) can be subject to the magnetorotational instability (MRI) and the vertical shear instability (VSI). While both processes can drive turbulence in the disk, existing numerical simulations have studied them separately. In this paper, we conduct global 3D non-ideal magnetohydrodynamic (MHD) simulations for outer PPDs with ambipolar diffusion and instantaneous cooling, and hence conductive to both instabilities. Given the range of ambipolar Elsässer numbers (Am) explored, it is found that the VSI turbulence dominates over the MRI when ambipolar diffusion is strong ($Am = 0.1$); the VSI and MRI can co-exist for $Am = 1$; and the VSI is overwhelmed by the MRI when ambipolar diffusion is weak ($Am = 10$). Angular momentum transport process is primarily driven by MHD winds, while viscous accretion due to MRI and/or VSI turbulence makes a moderate contribution in most cases. Spontaneous magnetic flux concentration and formation of annular substructures remain robust in strong ambipolar diffusion dominated disks ($Am \leq 1$) with the presence of the VSI. Ambipolar diffusion is the major contributor to the magnetic flux concentration phenomenon rather than advection.

9. A Population of Dipper Stars from the Transiting Exoplanet Survey Satellite Mission

Benjamin K. Capistrant, Melinda Soares-Furtado, Andrew Vanderburg, Marina Kounkel, Saul A. Rappaport, Mark Omohundro, Brian P. Powell, Robert Gagliano, Thomas Jacobs, Veselin B. Kostov, Martti H. Kristiansen, Daryll M. LaCourse, Allan R. Schmitt, Hans Martin Schwengeler, Ivan A. Terentev ★ Dipper stars are a classification of young stellar objects that exhibit dimming variability in their light curves, dropping in brightness by 10-50%, likely induced by occultations due to circumstellar disk material. This variability can be periodic, quasi-periodic, or aperiodic. Dipper stars have been discovered in young stellar associations via ground-based and space-based photometric surveys. We present the detection and characterization of the largest collection of dipper stars to date: 293 dipper stars, including 234 new dipper candidates. We have produced a catalog of these targets, which also includes young stellar variables that exhibit predominately bursting-like variability and symmetric variability (equal parts bursting and dipping). The total number of catalog sources is 414. These variable sources were found in a visual survey of TESS light curves, where dipping-like variability was observed. We found a typical age among our dipper sources of <5 Myr, with the age distribution peaking at 2 Myr, and a tail of the distribution extending to ages older than 20 Myr. Regardless of the age, our dipper candidates tend to exhibit infrared excess, which is indicative of the presence of disks. TESS is now observing the ecliptic plane, which is rich in young stellar associations, so we anticipate many more discoveries in the TESS dataset. A larger sample of dipper stars would enhance the census statistics of light curve morphologies and dipper ages.

10. Complex Organic Molecules Formation in Cold Cores on Stochastically Heated Grains

Long-Fei Chen, Qiang Chang, Yao Wang, Di Li ★ We investigate the roles of stochastic grain heating in the formation of complex organic molecules (COMs) in cold cores, where COMs have been detected. Two different types of grain-size distributions are used in the chemical models. The first one is the MRN distribution, and the second one considers grain coagulation to study its effects on the chemical evolution in these environments. The macroscopic Monte Carlo method is used to perform the two-phase chemical model simulations. We find that (1) grain coagulation can affect certain gas-phase species, such as CO_2 and N_2H^+, in the cold core environments, which can be attributed to the volatile precursors originating from the small grains with temperature fluctuations; (2) grains with radii around 4.6×10^{-3} μm contribute most to the production of COMs on dust grains under cold core conditions, while few species can be formed on even smaller grains with radii less than 2×10^{-3} μm; (3) COMs formed on stochastically heated grains could help explain the observed abundances of gas-phase COMs in cold cores.

11. CHEMOUT: CHEMical complexity in star-forming regions of the OUTer Galaxy III. Nitrogen isotopic ratios in the outer Galaxy

L. Colzi, D. Romano, F. Fontani, V. M. Rivilla, L. Bizzocchi, M. T. Beltrán, P. Caselli, D. Elia, L. Magrini ★ Nitrogen isotopic ratios are a key tool for tracing Galactic stellar nucleosynthesis. We present the first study of the $^{14}N/^{15}N$ abundance ratio in the outer regions of the Milky Way (namely, for galactocentric distances, R_{GC}, from 12 kpc up to 19 kpc), with the aim to study the stellar nucleosynthesis effects in the global Galactic trend. We analysed IRAM 30m observations towards a sample of 35 sources in the context of the CHEMical complexity in star-forming regions of the OUTer Galaxy (CHEMOUT) project. We derived the $^{14}N/^{15}N$ ratios from HCN and HNC for 14 and 3 sources, respectively, using the $J = 1$-0 rotational transition of $HN^{13}C$, $H^{15}NC$, $H^{13}CN$, and $HC^{15}N$. The results found in the outer Galaxy have been combined with previous measurements obtained in the inner Galaxy. We find an overall linear decreasing $H^{13}CN/HC^{15}N$ ratio with increasing R_{GC}. This translates to a parabolic $^{14}N/^{15}N$ ratio with a peak at 11 kpc. Updated Galactic chemical evolution models have been taken into account and compared with the observations. The parabolic trend of the $^{14}N/^{15}N$ ratio with R_{GC} can be naturally explained (i) by a model that assumes novae as the main ^{15}N producers on long timescales ($\geq$1 Gyr) and (ii) by updated stellar yields for low- and intermediate-mass stars.

12. The Great Planetary Heist: Theft and capture in star-forming regions

Emma C. Daffern-Powell, Richard J. Parker, Sascha P. Quanz ★ Gravitational interactions in star-forming regions are capable of disrupting and destroying planetary systems, as well as creating new ones. In particular, a planet can be stolen, where it is directly exchanged between passing stars during an interaction; or captured, where a planet is first ejected from its birth system and is free-floating for a period of time, before being captured by a passing star. We perform sets of direct N-body simulations of young, substructured star-forming regions, and follow their evolution for 10 Myr in order to determine how many planets are stolen and captured, and their respective orbital properties. We show that in high density star-forming regions, stolen and captured planets have distinct properties. The semimajor axis distribution of captured planets is significantly skewed to wider orbits compared to the semimajor axis distribution of stolen planets and planets that are still orbiting their parent star (preserved planets). However, the eccentricity and inclination distributions of captured and stolen planets are similar, but in turn very different to the inclination and eccentricity distributions of preserved planets. In low-density star-forming regions these differences are not as distinct but could still, in principle, be used to determine whether observed exoplanets have likely formed in situ or have been stolen or captured. We find that the initial degree of spatial and kinematic substructure in a star-forming region is as important a factor as the stellar density in determining whether a planetary system will be altered, disrupted, captured or stolen.

13. Thermophysical evolution of planetesimals in the Primordial Disk

Björn J. R. Davidsson ★ The Primordial Disk of small icy planetesimals, once located at 15-30 AU from the Sun, was disrupted by giant planet migration in the early Solar System. The Primordial Disk thereby became the source region of objects in the current-day Kuiper Belt, Scattered Disk, and Oort Cloud. I present the thermophysics code "Numerical Icy Minor Body evolUtion Simulator", or NIMBUS, and use it to study the thermophysical evolution of planetesimals in the Primordial Disk prior to its disruption. Such modelling is mandatory in order to understand the behaviour of dynamically new comets from the Oort Cloud, as well as the activity of Centaurs and short-period comets from the Scattered Disk, that return pre-processed to the vicinity of the Sun. I find that bodies in the midst of the Primordial Disk with diameters ranging 4-200 km lost all their CO ice on time-scales of order 0.1-10 Myr depending on size, through a combination of protosolar and long-lived radionuclide heating. CO and other hypervolatiles therefore require a less volatile host for their storage. I consider two possible hosts:

amorphous water ice and CO2 ice. Because of the high luminosity of the protosun, some Primordial Disk bodies may have sustained significant crystallisation, CO:CO2 segregation, and CO2 sublimation in the uppermost few tens of meters. I discuss how this may affect coma abundance ratios and distant activity in dynamically new comets.

14. The formation of clusters and OB associations in different density spiral arm environments

C. L. Dobbs, T. J. R. Bending, A. R. Pettitt, A. S. M. Buckner, M. R. Bate ★ We present simulations of the formation and evolution of clusters in spiral arms. The simulations follow two different spiral arm regions, and the total gas mass is varied to produce a range of different mass clusters. We find that including photoionizing feedback produces the observed cluster mass radius relation, increasing the radii of clusters compared to without feedback. Supernovae have little impact on cluster properties. We find that in our high density, high gas mass simulations, star formation is less affected by feedback, as star formation occurs rapidly before feedback has much impact. In our lowest gas density simulation, the resulting clusters are completely different (e.g. the number of clusters and their masses) to the case with no feedback. The star formation rate is also significantly suppressed. The fraction of stars in clusters in this model decreases with time flattening at about 20%. In our lowest gas simulation model, we see the formation of a star forming group with properties similar to an OB association, in particular similar to Orion Ia. We suggest that low densities, and stronger initial dynamics are conducive to forming associations rather than clusters. In all models cluster formation is complex with clusters merging and splitting. The most massive clusters which form have tended to undergo more mergers.

15. Accretion Burst Echoes as Probes of Protostellar Environments and Episodic Mass Assembly

Logan Francis, Doug Johnstone, Jeong-Eun Lee, Gregory J. Herczeg, Feng Long, Steve Mairs, Carlos Contreras-Peña, Gerald Moriarty-Schieven ★ Protostars likely accrete material at a highly time variable rate, however, measurements of accretion variability from the youngest protostars are rare, as they are still deeply embedded within their envelopes. Sub-mm/mm observations can trace the thermal response of dust in the envelope to accretion luminosity changes, allowing variations in the accretion rate to be quantified. In this paper, we present contemporaneous sub-mm/mm light curves of variable protostars in Serpens Main, as observed by the ALMA ACA, SMA, and JCMT. The most recent outburst of EC 53 (V371 Ser), an ~ 18 month periodic variable, is well-sampled in the SMA and JCMT observations. The SMA light curve of EC 53 is observed to peak weeks earlier and exhibit a stronger amplitude than at the JCMT. Stochastic variations in the ACA observations are detected for SMM 10 IR with a factor ~ 2 greater amplitude than as seen by the JCMT. We develop a toy model of the envelope response to accretion outbursts to show EC 53's light curves are plausibly explained by the delay associated with the light travel time across the envelope and the additional dilution of the JCMT response by the incorporation of cold envelope material in the beam. The larger JCMT beam can also wash out the response to rapid variations, which may be occurring for SMM 10 IR. Our work thus provides a valuable proof of concept for the usage of sub-mm/mm observations as a probe of both the underlying accretion luminosity variations and the protostellar environment.

16. Accretion and extinction variations in the low-mass pre-main sequence binary system WX Cha

Eleonora Fiorellino, Gabriella Zsidi, Agnes Kospal, Peter Abraham, Attila Bodi, Gaitee Hussain, Carlo F. Manara, Andras Pal ★ Light curves of young star systems show photometric variability due to different kinematic, and physical processes. One of the main contributors to the photometric variability is the changing mass accretion rate, which regulates the interplay between the forming young star and the protoplanetary disk. We collected high-resolution spectroscopy in eight different epochs, as well as ground-based and space-borne multi-epoch optical and infrared photometry of WX Cha, an M0 binary system, with an almost edge-on disk (i = 87degrees) in the Chamaeleon I star-forming region. Spectroscopic observations cover 72 days, the ground-based optical monitoring covers 42 days while space-borne TESS photometry extends for 56 days. The multi-wavelength light curves exhibit quasi-periodic variability of 0.35 - 0.53 mag in the near-infrared, and of 1.3 mag in g band. We studied the variability of selected emission lines that trace the accretion, computed the accretion luminosity and the mass accretion rate using empirical relations and obtained values of the accretion luminosity between 1.6 and 3.2 Lsun and mass accretion rate between $3.31\text{x}10^{-7}$ Msun/yr and $7.76\text{x}10^{-7}$ Msun/yr. Our results show that WX Cha is accreting at a rate larger than what is typical for T Tauri stars in the same star-forming region with the same stellar parameters. We theorize that this is due to the higher disk mass of WX Cha than what is usual for stars with similar stellar mass, and to the binary nature of the system. Daily changes in the accretion luminosity and in the extinction can explain the photometric variability.

17. The relation between the Mass Accretion Rate and the Disk Mass in Class I Protostars

Eleonora Fiorellino, Lukasz Tychoniec, Carlo F. Manara, Giovanni Rosotti, Simone Antoniucci, Fernando Cruz-Saenz de Miera, Agnes Kospal, Brunella Nisini ★ The evidence of a relation between the mass accretion rate and the disk mass is established for young, Class II pre-main sequence stars. This observational result opened an avenue to test theoretical models and constrain the initial conditions of the disk formation, fundamental in the understanding of the emergence of planetary systems. However, it is becoming clear that the planet formation starts even before the Class II stage, in disks around Class 0 and I protostars. We show for the first time evidence for a correlation between the mass accretion rate and the disk mass for a large sample of Class I young stars located in nearby ($<$ 500 pc) star-forming regions. We fit our sample, finding that the Class I objects relation has a slope flatter than Class II stars, and have higher mass accretion rates and disk masses. The results are put in context of the disk evolution models.

18. Different degrees of nitrogen and carbon depletion in the warm molecular layers of protoplanetary disks

Kenji Furuya, Seokho Lee, Hideko Nomura ★ Observations have revealed that the elemental abundances of carbon and oxygen in the warm molecular layers of some protoplanetary disks are depleted compared to those is the interstellar medium by a factor of 10-100. Meanwhile, little is known about nitrogen. To investigate the time evolution of nitrogen, carbon, and oxygen elemental abundances in disks, we develop a one-dimensional model that incorporates dust settling, turbulent diffusion of dust and ices, as well as gas-ice chemistry including the chemistry driven by stellar UV/X-rays and the galactic cosmic rays. We find that gaseous CO in the warm molecular layer is converted to CO2 ice and locked up near the midplane via the combination of turbulent mixing (i.e., the vertical cold finger effect) and ice chemistry driven by stellar UV photons. On the other hand, gaseous N2, the main nitrogen reservoir in the warm molecular layer, is less processed by ice chemistry, and exists as it is. Then the nitrogen depletion occurs solely by the vertical cold finger effect of N2. As the binding energy of N2 is lower than that of CO and CO2, the degree of nitrogen depletion is smaller than that of carbon and oxygen depletion, leading to higher elemental abundance of nitrogen than that of carbon and oxygen. This evolution occurs within 1 Myr and proceeds further, when the α parameter for the diffusion coefficient is 0.001. Consequently, the N2H+/CO column density ratio increases with time. How the vertical transport affects the midplane ice composition is briefly discussed.

19. The JCMT BISTRO Survey: Multi-wavelength polarimetry of bright regions in NGC 2071 in the far-infrared/submillimetre range, with POL-2 and HAWC+

L. Fanciullo, F. Kemper, K. Pattle, P. M. Koch, S. Sadavoy, S. Coudé, A. Soam, T. Hoang, T. Onaka, V. J. M. Le Gouellec, D. Arzoumanian, D. Berry, C. Eswaraiah, E. J. Chung, R. Furuya, C. L. H. Hull, J. Hwang, D. Johnstone, J. -h. Kang, K. H. Kim, F. Kirchschlager, V. Könyves, J. Kwon, W. Kwon, S. -P. Lai, C. W. Lee, T. Liu, A. -R. Lyo, I. Stephens, M. Tamura, X. Tang, D. Ward-Thompson, A. Whitworth, H. Shinnaga ★ Polarized dust emission is a key tracer in the study of interstellar medium and of star formation. The observed polarization, however, is a product of magnetic field structure, dust grain properties and grain alignment efficiency, as well as their variations in the line of sight, making it difficult to interpret polarization unambiguously. The comparison of polarimetry at multiple wavelengths is a possible way of mitigating this problem. We use data from HAWC+/SOFIA and from SCUBA-2/POL-2 (from the BISTRO survey) to analyse the NGC 2071 molecular cloud at 154, 214 and 850 μm. The polarization angle changes significantly with wavelength over part of NGC 2071, suggesting a change in magnetic field morphology on the line of sight as each wavelength best traces different dust populations. Other possible explanations are the existence of more than one polarization mechanism in the cloud or scattering from very large grains. The observed change of polarization fraction with wavelength, and the 214-to-154 μm polarization ratio in particular, are difficult to reproduce with current dust models under the assumption of uniform alignment efficiency. We also show that the standard procedure of using monochromatic intensity as a proxy for column density may produce spurious results at HAWC+ wavelengths. Using both long-wavelength (POL-2, 850 μm) and short-wavelength (HAWC+, $\lesssim 200\,\mu$m) polarimetry is key in obtaining these results. This study clearly shows the importance of multi-wavelength polarimetry at submillimeter bands to understand the dust properties of molecular clouds and the relationship between magnetic field and star formation.

20. GIARPS High-resolution Observations of T Tauri stars (GHOsT). IV. Accretion properties of the Taurus-Auriga young association

M. Gangi, S. Antoniucci, K. Biazzo, A. Frasca, B. Nisini, J. M. Alcalà, T. Giannini, C. F. Manara, A. Giunta, A. Harutyunyan, U. Munari, F. Vitali ★ In the framework of the GIARPS@TNG High-resolution Observations of T Tauri stars (GHOsT) project, we study the accretion properties of 37 Classical T Tauri Stars of the Taurus-Auriga star forming region (SFR) with the aim of characterizing their relation with the properties of the central star, of jets and disk winds, and of the global disk structure, in synergy with complementary ALMA millimiter observations. We derive stellar parameters, optical veiling, accretion luminosity (L_{acc}) and mass accretion rate ($\dot{M}_{acc}$) in a homogeneous and self-consistent way using high-resolution spectra acquired at the Telescopio Nazionale Galileo with the HARPS-N and GIANO spectrographs, and flux-calibrated based on contemporaneous low-resolution spectroscopic and photometric ancillary observations. The L_{acc}-$L_\star$, $\dot{M}_{acc}$-$M_\star$ and $\dot{M}_{acc}$-M_{disk} relationships of the Taurus sample are provided and compared with those of the coeval SFRs of Lupus and Chamaeleon I. Our results demonstrate the potential of contemporaneous optical and near-infrared high-resolution spectroscopy to simultaneously provide precise measurements of stellar and accretion/wind properties of young stars.

21. Nonlinear evolution of streaming instabilities in accreting protoplanetary disks

Chun-Yen Hsu, Min-Kai Lin ★ The streaming instability (SI) is one of the most promising candidates for triggering planetesimal formation by producing dense dust clumps that undergo gravitational collapse. Understanding how the SI operates in realistic protoplanetary disks (PPDs) is therefore crucial to assess the efficiency of planetesimal formation. Modern models of PPDs show that large-scale magnetic torques or winds can drive laminar gas accretion near the disk midplane. In a previous study, we identified a new linear dust-gas instability, the azimuthal drift SI (AdSI), applicable to such accreting disks and is powered by the relative azimuthal motion between dust and gas that results from the gas being torqued. In this work, we present the first nonlinear simulations of the AdSI. We show that it can destabilize an accreting, dusty disk even in the absence of a global radial pressure gradient, which is unlike the classic SI. We find the AdSI drives turbulence and the formation of vertically-extended dust filaments that undergo merging. In dust-rich disks, merged AdSI filaments reach maximum dust-to-gas ratios exceeding 100. Moreover, we find that even in dust-poor disks the AdSI can increase local dust densities by two orders of magnitude. We discuss the possible role of the AdSI in planetesimal formation, especially in regions of an accreting PPD with vanishing radial pressure gradients.

22. The hydrogen clock to infer the upper stellar mass

Erin R. Higgins, Jorick S. Vink, Gautham N. Sabhahit, Andreas A. C. Sander ★ The most massive stars dominate the chemical enrichment, mechanical and radiative feedback, and energy budget of their host environments. Yet how massive stars initially form and how they evolve throughout their lives is ambiguous. The mass loss of the most massive stars remains a key unknown in stellar physics, with consequences for stellar feedback and populations. In this work, we compare grids of very massive star (VMS) models with masses ranging from 80-1000Msun, for a range of input physics. We include enhanced winds close to the Eddington limit as a comparison to standard O-star winds, with consequences for present-day observations of 50-100Msun stars. We probe the relevant surface H abundances (Xs) to determine the key traits of VMS evolution compared to O stars. We find fundamental differences in the behaviour of our models with the enhanced-wind prescription, with a convergence on the stellar mass at 1.6 Myr, regardless of the initial mass. It turns out that Xs is an important tool in deciphering the initial mass due to the chemically homogeneous nature of VMS above a mass threshold. We use Xs to break the degeneracy of the initial masses of both components of a detached binary, and a sample of WNh stars in the Tarantula nebula. We find that for some objects, the initial masses are unrestricted and, as such, even initial masses of the order 1000Msun are not excluded. Coupled with the mass turnover at 1.6 Myr, Xs can be used as a 'clock' to determine the upper stellar mass.

23. ALMA Datacubes and Continuum Maps of the Irradiated Western Wall in Carina

Patrick Hartigan, Maxwell Hummel, Andrea Isella, Turlough Downes ★ We present ALMA observations of the continuum and line emission of ^{12}CO, ^{13}CO, $C^{18}O$, and [C I] for a portion of the G287.38-0.62 (Car 1-E) region in the Carina star-forming complex. The new data record how a molecular cloud responds on subarcsecond scales when subjected to a powerful radiation front, and provide insights into the overall process of star formation within regions that contain the most massive young stars. The maps show several molecular clouds superpose upon the line of sight, including a portion of the Western Wall, a highly-irradiated cloud situated near the young star cluster Trumpler 14. In agreement with theory, there is a clear progression from fluoresced H_2, to [C I], to $C^{18}O$ with distance into the PDR front. Emission from optically thick ^{12}CO extends across the region, while ^{13}CO, [C I] and especially $C^{18}O$ are more optically thin, and concentrate into clumps and filaments closer to the PDR interface. Within the Western Wall cloud itself we identify 254 distinct core-sized clumps in our datacube of $C^{18}O$. The mass distribution of these objects is similar to that of the stellar IMF. Aside from a large-scale velocity gradient, the clump radial velocities lack any spatial coherence size. There is no direct evidence for triggering of star formation in the Western Wall in that its $C^{18}O$ clumps and continuum cores appear starless, with no pillars present. However, the densest portion of the cloud lies closest to the PDR, and the $C^{18}O$ emission is flattened along the radiation front.

24. A gap at 1 au in the disk of DI Cha A revealed by infrared interferometry

Tímea Juhász, Péter Ábrahám, Attila Moór, Lei Chen, Ágnes Kóspál, József Varga, Zsolt Regály, Gabriella Zsidi, András Pál ★ DI Cha A is K0-type pre-main sequence star, the brightest component of a quadruple stellar system. Here we report on a detailed study of this star based on archival VLTI/MIDI and VLTI/PIONIER infrared interferometric observations, as well as optical–infrared photometric monitoring from ground-based and space-born instruments. We determined the structure of the circumstellar disk by fitting simultaneously the interferometric visibilities and the spectral energy distribution, using both analytical models and the radiative transfer code RADMC-3D. The modeling revealed that the radial density distribution of the disk appears to have a gap between 0.21 and 3.0 au. The inner ring, whose inner size coincides with the sublimation radius, is devoid of small, submicrometer-sized dust grains. The inner edge of the outer disk features a puffed-up rim, typically seen in intermediate-mass stars. Grain growth, although less progressed, was also detected in the outer disk. The inner ring is variable at mid-infrared wavelengths on both daily and annual timescales, while the star stays remarkably constant in the optical, pointing to geometrical or accretion changes in the disk as possible explanation for the flux variations.

25. Spectroscopic Confirmation of a Population of Isolated, Intermediate-Mass YSOs

Michael A. Kuhn, Ramzi Saber, Matthew S. Povich, Rafael S. de Souza, Alberto Krone-Martins, Emille E. O. Ishida, Catherine Zucker, Robert A. Benjamin, Lynne A. Hillenbrand, Alfred Castro-Ginard, Xingyu Zhou ★ Wide-field searches for young stellar objects (YSOs) can place useful constraints on the prevalence of clustered versus distributed star formation. The Spitzer/IRAC Candidate YSO (SPICY) catalog is one of the largest compilations of such objects (120,000 candidates in the Galactic midplane). Many SPICY candidates are spatially clustered, but, perhaps surprisingly, approximately half the candidates appear spatially distributed. To better characterize this unexpected population and confirm its nature, we obtained Palomar/DBSP spectroscopy for 26 of the optically-bright (G<15 mag) "isolated" YSO candidates. We confirm the YSO classifications of all 26 sources based on their positions on the Hertzsprung-Russell diagram, H and Ca II line-emission from over half the sample, and robust detection of infrared excesses. This implies a contamination rate of <10% for SPICY stars that meet our optical selection criteria. Spectral types range from B4 to K3, with A-type stars most common. Spectral energy distributions, diffuse interstellar bands, and Galactic extinction maps indicate moderate to high extinction. Stellar masses range from 1 to 7 $M_\odot$, and the estimated accretion rates, ranging from 3×10^{-8} to 3×10^{-7} $M_\odot$ yr^{-1}, are typical for YSOs in this mass range. The 3D spatial distribution of these stars, based on Gaia astrometry, reveals that the "isolated" YSOs are not evenly distributed in the Solar neighborhood but are concentrated in kpc-scale dusty Galactic structures that also contain the majority of the SPICY YSO clusters. Thus, the processes that produce large Galactic star-forming structures may yield nearly as many distributed as clustered YSOs.

26. MHD simulations of dense core collision

Shinichi W. Kinoshita, Fumitaka Nakamura ★ We investigated the effect of magnetic fields on the collision process between dense molecular cores. We performed three-dimensional magnetohydrodynamic simulations of collisions between two self-gravitating cores using the Enzo adaptive mesh refinement code. The core was modeled as a stable isothermal Bonnor-Ebert (BE) sphere immersed in uniform magnetic fields. Collisions were characterized by the offset parameter b, Mach number of the initial core $\mathcal{M}$, magnetic field strength B_0, and angle θ between the initial magnetic field and collision axis. For head-on ($b = 0$) collisions, one protostar was formed in the compressed layer. The higher the magnetic field strength, the lower the accretion rate. For models with $b = 0$ and $\theta = 90°$, the accretion rate was more dependent on the initial magnetic field strength compared with $b = 0$ and $\theta = 0°$ models. For off-center ($b = 1$) collisions, the higher specific angular momentum increased; therefore, the gas motion was complicated. In models with $b = 1$ and $\mathcal{M} = 1$, the number of protostars and gas motion highly depended on B_0 and θ. For models with $b = 1$ and $\mathcal{M} = 3$, no significant shock-compressed layer was formed and star formation was not triggered.

27. Primordial Dusty Rings and Episodic Outbursts in Protoplanetary Discs

Kundan Kadam, Eduard Vorobyov, Shantanu Basu ★ We investigate the formation and evolution of "primordial" dusty rings occurring in the inner regions of protoplanetary discs, with the help of long-term, coupled dust-gas, magnetohydrodynamic simulations. The simulations are global and start from the collapse phase of the parent cloud core, while the dead zone is calculated via an adaptive α formulation by taking into account the local ionization balance. The evolution of the dusty component includes its growth and back reaction on to the gas. Previously, using simulations with only a gas component, we showed that dynamical rings form at the inner edge of the dead zone. We find that when dust evolution as well as magnetic field evolution in the flux-freezing limit are included, the dusty rings formed are more numerous and span a larger radial extent in the inner disc, while the dead zone is more robust and persists for a much longer time. We show that these dynamical rings concentrate enough dust mass to become streaming unstable, which should result in rapid planetesimal formation even in the embedded phases of the system. The episodic outbursts caused by the magnetorotational instability have significant impact on the evolution of the rings. The outbursts drain the inner disc of grown dust, however, the period between bursts is sufficiently long for the planetesimal growth via streaming instability.The dust mass contained within the rings is large enough to ultimately produce planetary systems with the core accretion scenario. The low mass systems rarely undergo outbursts and thus, the conditions around such stars can be especially conducive for planet formation.

28. Massive young stellar objects in the Local Group spiral galaxy M33 identified using machine learning

David A. Kinson, Joana M. Oliveira, Jacco Th. van Loon ★ We present a supervised machine learning classification of stellar populations in the Local Group spiral galaxy M 33. The Probabilistic Random Forest (PRF) methodology, previously applied to populations in NGC 6822, utilises both near and far-IR classification features. It classifies sources into nine target classes: young stellar objects (YSOs), oxygen- and carbon-rich asymptotic giant branch stars, red giant branch and red supergiant stars, active galactic nuclei, blue stars (e.g. O-, B- and A-type main sequence stars), Wolf-Rayet stars and Galactic foreground stars. Across 100 classification runs the PRF classified 162,746 sources with an average estimated accuracy of ~ 86 per cent, based on confusion matrices. We identified 4985 YSOs across the disk of M 33, applying a density-based clustering analysis to identify 68 star forming regions (SFRs) primarily in the galaxy's spiral arms. SFR counterparts to known H II regions were recovered, with ~ 91 per cent of SFRs spatially coincident with giant molecular clouds identified in the literature. Using photometric measurements, as well as SFRs in NGC 6822 with an established evolutionary sequence as a benchmark, we employed a novel approach combining ratios of [Hα]/[24μm] and [250μm]/[500μm] to estimate the relative evolutionary status of all M 33 SFRs. Masses were estimated for each YSO ranging from $6-27\,\mathrm{M}_\odot$. Using these masses, we estimate star formation rates based on direct YSO counts of $0.63\,\mathrm{M}_\odot\,\mathrm{yr}^{-1}$ in M 33's SFRs, $0.79 \pm 0.16\,\mathrm{M}_\odot\,\mathrm{yr}^{-1}$ in its centre and $1.42 \pm 0.16\,\mathrm{M}_\odot\,\mathrm{yr}^{-1}$ globally.

29. Role of Filamentary Structures in the Formation of Two Dense Cores, L1544 and L694-2

Shinyoung Kim, Chang Won Lee, Mario Tafalla, Maheswar Gophinathan, Paola Caselli, Philip C. Myers, Eun Jung Chung, Shanghuo Li ★ We present mapping results of two prestellar cores, L1544 and L694-2, embedded in filamentary clouds in $C^{18}O$ (3-2), ^{13}CO (3-2), ^{12}CO (3-2), HCO^+ (4-3), and $H^{13}CO^+$ (4-3) with the JCMT telescope to examine the role of the filamentary structures in the formation of dense cores in the clouds, with new distance estimates for L1544 (175^{+4}_{-3} pc) and L694-2 (203^{+6}_{-7} pc). From these observations, we found that the non-thermal velocity dispersion of two prestellar cores and their surrounding clouds are smaller than or comparable to the sound speed. This may indicate that the turbulence has already been dissipated for both filaments and cores during their formation time. We also found a $\lambda/4$ shift between the periodic oscillations in the velocity and the column density distributions implying the possible presence of gravitational core-forming flow motion along the axis of the filament. The mass accretion rates due to these flow motions are estimated to be 2-3 $\mathrm{M}_\odot$ Myr^{-1}, being comparable to that for Serpens cloud but much smaller than those for the Hub filaments, cluster, or high mass forming filaments by 1 or 2 order of magnitudes. From this study, we suggest that the filaments in our targets might be formed from the shock-compression of colliding clouds, and then the cores are formed by gravitational fragmentation of the filaments to evolve to the prestellar stage. We conclude that the filamentary structures in the clouds play an important role in the entire process of formation of dense cores and their evolution.

30. Isolated Massive Star Formation in G28.20-0.05

Chi-Yan Law, Jonathan C. Tan, Prasanta Gorai, Yichen Zhang, Rubén Fedriani, Daniel Tafoya, Kei Tanaka, Giuliana Cosentino, Yao-Lun Yang, Diego Mardones, Maria Teresa Beltrán, Guido Garay ★ We report high-resolution 1.3 mm continuum and molecular line observations of the massive protostar G28.20-0.05 with ALMA. The continuum image reveals a ring-like structure with 2,000 au radius, similar to morphology seen in archival 1.3 cm VLA observations. Based on its spectral index and associated H30α emission, this structure mainly traces ionised gas. However, there is evidence for $\sim 30\,\mathrm{M}_\odot$ of dusty gas near the main mm continuum peak on one side of the ring, as well as in adjacent regions within 3,000 au. A virial analysis on scales of $\sim$2,000 au from hot core line emission yields a dynamical mass of $\sim 80\,M_\odot$. A strong velocity gradient in the H30α emission is evidence for a rotating, ionized disk wind, which drives a larger-scale molecular outflow. An infrared SED analysis indicates a current protostellar mass of $m_* \sim 40\,M_\odot$ forming from a core with initial mass $M_c \sim 300\,M_\odot$ in a clump with mass surface density of $\Sigma_{\rm cl} \sim 0.8\,\mathrm{g\,cm^{-2}}$. Thus the SED and other properties of the system can be understood in the context of core accretion models. Structure-finding analysis on the larger-scale continuum image indicates G28.20-0.05 is forming in a relatively isolated environment, with no other concentrated sources, i.e., protostellar cores, above $\sim 1\,M_\odot$ found from $\sim$0.1 to 0.4 pc around the source. This implies that a massive star can form in relative isolation and the dearth of other protostellar companions within the ~ 1 pc environs is a strong constraint on massive star formation theories that predict the presence of a surrounding protocluster.

31. Diagnosing FUor-like Sources: The Parameter Space of Viscously Heated Disks in the Optical and Near-IR

Hanpu Liu, Gregory J. Herczeg, Doug Johnstone, Carlos Contreras-Peña, Jeong-Eun Lee, Haifeng Yang, Xingyu Zhou, Sung-Yong Yoon, Ho-Gyu Lee, Masanobu Kunitomo, Jessy Jose ★ FU Ori type objects (FUors) are decades-long outbursts of accretion onto young stars that are strong enough to viscously heat disks so that the disk outshines the central star. We construct models for FUor objects by calculating emission components from a steady-state viscous accretion disk, a passively-heated dusty disk, magnetospheric accretion columns, and the stellar photosphere. We explore the parameter space of the accretion rate and stellar mass to investigate implications on the optical and near-infrared spectral energy distribution and spectral lines. The models are validated by fitting to multi-wavelength photometry of three confirmed FUor objects, FU Ori, V883 Ori and HBC 722 and then comparing the predicted spectrum to observed optical and infrared spectra. The brightness ratio between the viscous disk and the stellar photosphere, η, provides an important guide for identifying viscous accretion disks, with $\eta = 1$ ("transition line") and $\eta = 5$ ("sufficient dominance line") marking turning points in diagnostics, evaluated here in the near-infrared. These turning points indicate the emergence and complete development of FUor-characteristic strong CO absorption, weak metallic absorption, the triangular spectral continuum shape in the H-band, and location in color-magnitude diagrams. Lower stellar mass M_* and higher accretion rate $\dot{M}$ lead to larger η; for $M_* = 0.3$ $M_\odot$, $\eta = 1$ corresponds to $\dot{M} = 2 \times 10^{-7}$ $M_\odot$/yr and $\eta = 5$ to $\dot{M} = 6 \times 10^{-7}$ $M_\odot$/yr. The sufficient dominance line also coincides with the expected accretion rate where accreting material directly reaches the star. We discuss implications of the models on extinction diagnostics, FUor brightening timescales, viscous disks during initial protostellar growth, and eruptive young stellar objects (YSO) associated with FUors.

32. On The Unusual Variability of 2MASS J06195260-2903592: A Long-Lived Disk around a Young Ultracool Dwarf

Michael C. Liu, Eugene A. Magnier, Eric Gaidos, Trent J. Dupuy, Pengyu Liu, Beth A. Biller, Johanna M. Vos, Katelyn N. Allers, Jason T. Hinkle, Benjamin J. Shappee, Sage N. L. Constantinou, Mitchell T. Dennis, Kenji S. Emerson ★ We present the characterization of the low-gravity M6 dwarf 2MASS J0619-2903 previously identified as an unusual field object based on its strong IR excess and variable near-IR spectrum. Multiple epochs of low-resolution (R 150) near-IR spectra show large-amplitude (0.1-0.5 mag) continuum variations on timescales of days to 12 years, unlike the small-amplitude variability typical for field ultracool dwarfs. The variations between epochs are well-modeled as changes in the relative extinction ($\Delta A_V \approx 2$ mag). Likewise, Pan-STARRS optical photometry varies on timescales as long as 11 years (and possibly as short as an hour) and implies similar amplitude A_V changes. NEOWISE mid-IR light curves also suggest changes on 6-month timescales, with amplitudes consistent with the optical/near-IR extinction variations. However, near-IR spectra, near-IR photometry, and optical photometry obtained in the past year indicate the source can also be stable on hourly and monthly timescales. From comparison to objects of similar spectral type, the total extinction of 2MASS J0619-2903 seems to be $A_V \approx 4-6$ mag, with perhaps epochs of lower extinction. Gaia EDR3 finds that 2MASS J0619-2903 has a wide-separation (1.2' = 10450 AU) stellar companion, with an isochronal age of 31^{+22}_{-10} Myr and a mass of $0.30^{+0.04}_{-0.03}$ Msun. Adopting this companion's age and EDR3 distance (145.2±0.6 pc), we estimate a mass of 0.11-0.17 Msun for 2MASS J0619-2903. Altogether, 2MASS J0619-2903 appears to possess an unusually long-lived primordial circumstellar disk, perhaps making it a more obscured analog to the "Peter Pan" disks found around a few M dwarfs in nearby young moving groups.

33. ALMA Detection of Dust Trapping around Lagrangian Points in the LkCa 15 Disk

Feng Long, Sean M. Andrews, Shangjia Zhang, Chunhua Qi, Myriam Benisty, Stefano Facchini, Andrea Isella, David J. Wilner, Jaehan Bae, Jane Huang, Ryan A. Loomis, Karin I. Öberg, Zhaohuan Zhu ★ We present deep high-resolution (∼50 mas, 8 au) ALMA 0.88 and 1.3 mm continuum observations of the LkCa 15 disk. The emission morphology shows an inner cavity and three dust rings at both wavelengths, but with slightly narrower rings at the longer wavelength. Along a faint ring at 42 au, we identify two excess emission features at $\sim 10\sigma$ significance at both wavelengths: one as an unresolved clump and the other as an extended arc, separated by roughly 120 degrees in azimuth. The clump is unlikely to be a circumplanetary disk (CPD) as the emission peak shifts between the two wavelengths even after accounting for orbital motion. Instead, the morphology of the 42 au ring strongly resembles the characteristic horseshoe orbit produced in planet–disk interaction models, where the clump and the arc trace dust accumulation around Lagrangian points L_4 and L_5, respectively. The shape of the 42 au ring, dust trapping in the outer adjacent ring, and the coincidence of the horseshoe ring location with a gap in near-IR scattered light, are all consistent with the scenario of planet sculpting, with the planet likely having a mass between those of Neptune and Saturn. We do not detect point-like emission associated with a CPD around the putative planet location ($0.''27$ in projected separation from the central star at a position angle of ∼60 deg), with upper limits of 70 and 33 μJy at 0.88 and 1.3 mm, respectively, corresponding to dust mass upper limits of 0.02–0.03 $M_\oplus$.

34. BFS 10: A nascent bipolar H II region in a filamentary molecular cloud

Nicholas Larose, C. R. Kerton ★ We present a study of the compact blister HII region BFS 10 and its highly filamentary molecular cloud. We utilize 12CO observations from the Five College Radio Astronomy Observatory to determine the distance, size, mass, and velocity structure of the molecular cloud. Infrared observations obtained from the UKIRT Infrared Deep Sky Survey and the Spitzer Infrared Array Camera, as well as radio continuum observations from the Canadian Galactic Plane Survey, are used to extract information about the central HII region. This includes properties such as the ionizing photon rate and infrared luminosity, as well as identifying a rich embedded star cluster associated with the central O9 V star. Time-scales regarding the expansion rate of the HII region and lifetime of the ionizing star reveal a high likelihood that BFS 10 will develop into a bipolar HII region. Although the region is expected to become bipolar, we conclude from the clouds velocity structure that there is no evidence to support the idea that star formation at the location of BFS 10 was triggered by two colliding clouds. A search for embedded young stellar objects (YSOs) within the molecular cloud was performed. Two distinct regions of YSOs were identified; one region associated with the rich embedded cluster and another sparse group associated with an intermediate mass YSO.

35. The ALMA Survey of 70 μm Dark High-mass Clumps in Early Stages (ASHES). VII: Chemistry of Embedded Dense Cores

Shanghuo Li, Patricio Sanhueza, Xing Lu, Chang Won Lee, Qizhou Zhang, Stefano Bovino, Giovanni Sabatini, Tie Liu, Kee-Tae Kim, Kaho Morii, Daniel Tafoya, Ken'ichi Tatematsu, Takeshi Sakai, Junzhi Wang, Fei Li, Andrea Silva, Natsuko Izumi, David Allingham ★ We present a study of chemistry toward 294 dense cores in 12 molecular clumps using the data obtained from the ALMA Survey of 70 μm dark High-mass clumps in Early Stages (ASHES). We identified 97 protostellar cores and 197 prestellar core candidates based on the detection of outflows and molecular transitions of high upper energy levels ($E_u/k > 45$ K). The detection rate of the N_2D^+ emission toward the protostellar cores is 38%, which is higher than 9% for the prestellar cores, indicating that N_2D^+ does not exclusively trace prestellar cores. The detection rates of the DCO^+ emission are 35% for the prestellar cores and 49% for the protostellar cores, which are higher than those of N_2D^+, implying that DCO^+ appears more frequently than N_2D^+ in both prestellar and protostellar cores. Both N_2D^+ and DCO^+ abundances appear to decrease from the prestellar to protostellar stage. The DCN, C_2D and ^{13}CS emission lines are rarely seen in the dense cores of early evolutionary phases. The detection rate of the H_2CO emission toward dense cores is 52%, three times higher than that of CH_3OH (17%). In addition, the H_2CO detection rate, abundance, line intensities, and line widths increase with the core evolutionary status, suggesting that the H_2CO line emission is sensitive to protostellar activity.

36. The evolution of protoplanetary disc radii and disc masses in star-forming regions

Bridget Marchington, Richard J. Parker ★ Protoplanetary discs are crucial to understanding how planets form and evolve, but these objects are subject to the vagaries of the birth environments of their host stars. In particular, photoionising radiation from massive stars has been shown to be an effective agent in disrupting protoplanetary discs. External photoevaporation leads to the inward evolution of the radii of discs, whereas the internal viscous evolution of the disc causes the radii to evolve outwards. We couple N-body simulations of star-forming regions with a post-processing analysis of disc evolution to determine how the radius and mass distributions of protoplanetary discs evolve in young star-forming regions. To be consistent with observations, we find that the initial disc radii must be of order 100au, even though these discs are readily destroyed by photoevaporation from massive stars. Furthermore, the observed disc radii distribution in the Orion Nebula Cluster is more consistent with moderate initial stellar densities ($100 M_\odot$ pc^{-3}), in tension with dynamical models that posit much higher inital densities for the ONC. Furthermore, we cannot reproduce the observed disc radius distribution in the Lupus star-forming region if its discs are subject to external photoevaporation. A more detailed comparison is not possible due to the well-documented uncertainties in determining the ages of pre-main sequence (disc-hosting) stars.

37. Recent progress with observations and models to characterize the magnetic fields from star-forming cores to protostellar disks

Anaëlle Maury, Patrick Hennebelle, Josep Miquel Girart ★ In this review paper, we aim at providing a global outlook on the progresses made in the recent years to characterize the role of magnetic fields during the embedded phases of the star formation process. Thanks to the development of observational capabilities and the parallel progress in numerical models capturing most of the important physics at work during star formation, it has recently become possible to confront detailed predictions of magnetized models to observational properties of the youngest protostars. We provide an overview of the most important consequences when adding magnetic fields to state-of-the-art models of protostellar formation, emphasizing their role to shape the resulting star(s) and their disk(s). We discuss the importance of magnetic field coupling to set the efficiency of magnetic processes, and provide a review of observational works putting constraints on the two main agents responsible for the coupling in star-forming cores: dust grains and ionized gas. We recall the physical processes and observational methods allowing to trace the magnetic field topology and its intensity in embedded protostars, and review the main steps, success and limitations in comparing real observations to synthetic observations from the non-ideal MHD models. Finally, we discuss the main threads of observational evidence that suggest a key role of magnetic fields for star and disk formation, and propose a scenario solving the angular momentum for star formation, also highlighting the remaining tensions that exist between models and observations.

38. ArTéMiS imaging of the filamentary infrared dark clouds G1.75-0.08 and G11.36+0.80: Dust-based physical properties of the clouds and their clumps

Oskari Miettinen, Michael Mattern, Philippe André ★ We imaged the infrared dark clouds (IRDCs) G1.75-0.08 and G11.36+0.80 at 350 μm and 450 μm using the ArTéMiS bolometer. These data were used in conjunction with our previous 870 μm observations with the Large APEX BOlometer CAmera (LABOCA). The clumps in G11.36+0.80 were also observed in the $N_2H^+(1-0)$ transition with the IRAM 30-metre telescope. G1.75-0.08 was found to be composed of two cold ($\sim$ 14.5 K), massive (several $\sim 10^3$ M$_\odot$) clumps that are projectively separated by $\sim$ 3.7 pc. Both clumps are 70 μm dark, but they do not appear to be bounded by self-gravity. The G1.75-0.08 filament was found to be subcritical by a factor of $\sim$ 14 with respect to its critical line mass. G11.36+0.80 was found to be moderately (by a factor of $\sim$ 2) supercritical and composed of four clumps. The dust temperatures of the clumps are $\sim 13-15$ K, and their masses are in the range $\sim 232-633$ M$_\odot$. All the clumps are gravitationally bound. The projected, average separation of the clumps is $\sim$ 1 pc. A configuration that is observed in G1.75-0.08, namely two clumps at the ends of the filament, could be the result of gravitational focussing acting along the cloud. The two clumps fulfil the mass-radius threshold for high-mass star formation. Owing to the location of G1.75-0.08 near the Galactic centre ($\sim$ 270 pc), environmental effects such as a high level of turbulence, tidal forces, and shearing motions could affect the cloud dynamics. The observed clump separation in G11.36+0.80 can be understood in terms of a sausage instability. The G11.36+0.80 clumps do not lie above the mass-radius threshold for high-mass star formation. The substructure observed in one of the clumps in G11.36+0.80 suggests that the IRDC has fragmented in a hierarchical fashion. This conforms to the filamentary paradigm for Galactic star formation.

39. A millimeter-multiwavelength continuum study of VLA 1623 West

Arnaud Michel, Sarah I. Sadavoy, Patrick D. Sheehan, Leslie W. Looney, Erin G. Cox ★ VLA 1623 West is an ambiguous source that has been described as a shocked cloudlet as well as a protostellar disk. We use deep ALMA 1.3 and 0.87 millimeter observations to constrain its shape and structure to determine its origins better. We use a series of geometric models to fit the uv visibilities at both wavelengths with GALARIO. Although the Real visibilities show structures similar to what has been identified as gaps and rings in protoplanetary disks, we find that a modified Flat-Topped Gaussian at high inclination provides the best fit to the observations. This fit agrees well with expectations for an optically thick, highly inclined disk. Nevertheless, we find that the geometric models consistently yield positive residuals at the four corners of the disk at both wavelengths. We interpret these residuals as evidence that the disk is flared in the millimeter dust. We use a simple toy model for an edge-on flared disk and find that the residuals best match a disk with flaring that is mainly restricted to the outer disk at $R \gtrsim 30$ au. Thus, VLA 1623W may represent a young protostellar disk where the large dust grains have not yet had enough time to settle into the mid-plane. This result may have implications for how disk evolution and vertical dust settling impact the initial conditions leading to planet formation.

40. Snapshot of a magnetohydrodynamic disk wind traced by water maser observations

Luca Moscadelli, Alberto Sanna, Henrik Beuther, André Oliva, Rolf Kuiper ★ The formation of astrophysical objects of different nature and size, from black holes to gaseous giant planets, involves a disk-jet system, where the disk drives the mass accretion onto a central compact object and the jet is a fast collimated ejection along the disk rotation axis. Magnetohydrodynamic disk winds can provide the link between mass accretion and ejection, which is essential to ensure that the excess angular momentum is removed from the system and accretion onto the central object can proceed. However, up to now, we have been lacking direct observational proof of disk winds. This work presents a direct view of the velocity field of a disk wind around a forming massive star. Achieving a very high spatial resolution of 0.05 au, our water maser observations trace the velocities of individual streamlines emerging from the disk orbiting the forming star. We find that, at low elevation above the disk midplane, the flow co-rotates with its launch point in the disk, in agreement with magneto-centrifugal acceleration where the gas is flung away along the magnetic field line anchored to the disk. Beyond the co-rotation point, the flow rises spiraling around the disk rotation axis along a helical magnetic field. We have performed (resistive-radiative-gravito-) magnetohydrodynamic simulations of the formation of a massive star and record the development of a magneto-centrifugally launched jet presenting many properties in agreement with our observations.

41. Could kilomasers pinpoint supermassive stars?

Katarzyna Nowak, Martin. G. H. Krause, Daniel Schaerer ★ A strong nuclear kilomaser, W1, has been found in the nearby galaxy NGC 253, associated with a forming super star cluster. Kilomasers could arise from the accretion disc around supermassive stars ($> 10^3$ Msun), hypothetical objects that have been proposed as polluters responsible for the chemical peculiarities in globular clusters. The supermassive stars would form via runaway collisions, simultaneously with the cluster. Their discs are perturbed by stellar flybys, inspiralling and colliding stars. This raises the question if an accretion disc would at all be able to survive in such a dynamic environment and mase water lines. We investigated what the predicted maser spectrum of such a disc would look like using 2D hydrodynamic simulations and compared this to the W1 kilomaser. We derived model maser spectra from the simulations by using a general maser model for appropriate disc temperatures. All our model discs survived. The model maser spectra for the most destructive case for the simulations of M = 1000 Msun are a reasonable match with the W1 kilomaser spectrum in terms of scaling, flux values and some of the signal trends. Details in the spectrum suggest that a star of a few 1000 Msun might fit even better, with 10,000 Msun clearly giving too large velocities. Our investigations thus support the hypothesis that kilomasers could pinpoint supermassive stars.

42. Sequential Star Formation in the Young SMC Region NGC 602: Insights from ALMA

Theo J. O'Neill, Remy Indebetouw, Karin Sandstrom, Alberto D. Bolatto, Katherine E. Jameson, Lynn R. Carlson, Molly K. Finn, Margaret Meixner, Elena Sabbi, Marta Sewilo ★ NGC 602 is a young, low-metallicity star cluster in the "Wing" of the Small Magellanic Cloud. We reveal the recent evolutionary past of the cluster through analysis of high-resolution (∼0.4 pc) Atacama Large Millimeter/submillimeter Array observations of molecular gas in the associated HII region N90. We identify 110 molecular clumps ($R < 0.8$ pc) traced by CO emission, and study the relationship between the clumps and associated young stellar objects (YSOs) and pre-main-sequence (PMS) stars. The clumps have high virial parameters (typical $\alpha_{\rm vir}$ = 4-11) and may retain signatures of a collision in the last $\lesssim$8 Myr between HI components of the adjacent supergiant shell SMC-SGS 1. We obtain a CO-bright-to-H_2 gas conversion factor of $X_{CO,B} = (3.4 \pm 0.2) \times 10^{20}$ cm^{-2} (K km $s^{-1})^{-1}$, and correct observed clump properties for CO-dark H_2 gas to derive a total molecular gas mass in N90 of $16,600 \pm 2,400$ $M_\odot$. We derive a recent ($\lesssim$ 1 Myr) star formation rate of 130 ± 30 $M_\odot$ Myr^{-1} with an efficiency of $8 \pm 3\%$ assessed through comparing total YSO mass to total molecular gas mass. Very few significant radial trends exist between clump properties or PMS star ages and distance from NGC 602. We do not find evidence for a triggered star formation scenario among the youngest ($\lesssim$2 Myr) stellar generations, and instead conclude that a sequential star formation process in which NGC 602 did not directly cause recent star formation in the region is likely.

43. Depletion of gaseous CO in protoplanetary disks by surface-energy-regulated ice formation

Diana Powell, Peter Gao, Ruth Murray-Clay, Xi Zhang ★ Empirical constraints of fundamental properties of protoplanetary disks are essential for understanding planet formation and planetary properties (1,2). Carbon monoxide (CO) gas is often used to constrain disk properties (3). However, estimates show that the CO gas abundance in disks is depleted relative to expected values (4,5,6,7), and models of various disk processes impacting the CO abundance could not explain this depletion on observed 1Myr timescales (8,9,10,11,12,13,14). Here we demonstrate that surface energy effects on particles in disks, such as the Kelvin effect, that arise when ice heterogeneously nucleates onto an existing particle can efficiently trap CO in its ice phase. In previous ice formation models, CO gas was released when small ice-coated particles were lofted to warmed disk layers. Our model can reproduce the observed abundance, distribution and time evolution of gaseous CO in the four most studied protoplanetary disks (7). We constrain the solid and gaseous CO inventory at the midplane and disk diffusivities and resolve inconsistencies in estimates of the disk mass – three crucial parameters that control planetary formation.

44. Binding Energies of Interstellar Relevant S-bearing Species on Water Ice Mantles: A Quantum Mechanical Investigation

J. Perrero, J. Enrique-Romero, S. Ferrero, C. Ceccarelli, L. Podio, C. Codella, A. Rimola, P. Ugliengo ★ Binding energies (BEs) are one of the most important parameters for astrochemical modeling determining, because they govern whether a species stays in the gas-phase or is frozen on the grain surfaces. It is currently known that, in the denser and colder regions of the interstellar medium, sulphur is severely depleted in the gas phase. It has been suggested that it may be locked into the grain icy mantles. However, which are the main sulphur carriers is still a matter of debate. This work aims at establishing accurate BEs of 17 sulphur-containing species on two validated water ice structural models, the proton-ordered crystalline (010) surface and an amorphous water ice surface. We adopted Density Functional Theory (DFT)-based methods (the hybrid B3LYP-D3(BJ) and the hybrid meta-GGA M06-2X functionals) to predict structures and energetics of the adsorption complexes. London's dispersion interactions are shown to be crucial for an accurate estimate of the BEs due to the presence of the high polarizable sulphur element. While on the crystalline model the adsorption is restricted to a very limited number of binding sites with single valued BEs, on the amorphous model several adsorption structures are predicted, giving a BE distribution for each species. With the exception of few cases, both experimental and other computational data are in agreement with our calculated BE values. A final discussion on how useful the computed BEs are with respect to the snow lines of the same species in protoplanetary disks is provided

45. Jet from the enigmatic high-latitude star BP Psc and evolutionary status of its driving source

I. S. Potravnov, M. Yu. Khovritchev, S. A. Artemenko, D. N. Shakhovskoy ★ BP Psc is an active late-type (sp:G9) star with unclear evolutionary status lying at high galactic latitude $b = -57^{\circ}$. It is also the source of the well collimated bipolar jet. We present results of the proper motion and radial velocity study of BP Psc outflow based on the archival $H\alpha$ imaging with the GMOS camera at 8.1-m Gemini-North telescope as well as recent imaging and long-slit spectroscopy with the SCORPIO multi-mode focal reducer at 6-m BTA telescope of SAO RAS. The 3D kinematics of the jet revealed the full spatial velocity up to $\sim$140 km$\cdot$s^{-1} and allows us to estimate the distance to BP Psc system as $D = 135 \pm 40$ pc. This distance leads to an estimation of the central source luminosity $L_{*} \approx 1.2 L_{\odot}$, indicating that it is the $\approx$1.3$M_{\odot}$ T Tauri star with an age $t \lesssim 7$ Myr. We measured the electron density of order $N_e \sim 10^2$ cm^{-3} and mean ionization fraction $f \approx 0.04$ within the jet knots and estimated upper limit of the mass-loss rate in NE lobe as $\dot{M}_{out} \approx 1.2 \cdot 10^{-8} M_{\odot} \cdot yr^{-1}$. The physical characteristics of the outflow are typical for the low-excitation YSO jets and consistent with the magnetocentrifugal mechanism of its launching and collimation. Prominent wiggling pattern revealed in $H\alpha$ images allowed us to suppose the existence of a secondary substellar companion in a non-coplanar orbit and estimate its most plausible mass as $M_p \approx 30 M_{Jup}$. We conclude that BP Psc is one of the closest to the Sun young jet-driving systems and its origin is possibly related to the episode of star formation triggered by expanding supershells in Second Galactic quadrant.

46. Star and Cluster Formation in the Sh2-112 Filamentary Cloud Complex

Alik Panja, Yan Sun, Wen Ping Chen, Soumen Mondal ★ We present the star formation activity around the emission nebula Sh2-112. At a distance of $\sim$ 2.1 kpc, this ion H2 complex, itself 3 pc in radius, is illuminated by the massive star (O8 V) BD+45 3216. The associated molecular cloud extends in angular scales of 2.0×0.83, corresponding to linear sizes of 73 pc by 30 pc, along the Galactic longitude. The high-resolution (30 arcsec) extinction map reveals a chain of dust clumps aligned with the filament-like structure with an average extinction of $A_V \sim 2.78$ mag, varying up to a maximum of $\sim$ 17 mag. Our analysis led to identification of a rich population ($\sim$ 500) of young (average age of $\sim$ 1 Myr) stars, plus a numerous number ($\sim$ 350) of Hα emitters, spatially correlated with the filamentary clouds. Located near the edge of the cloud, the luminous star BD+45 3216 has created an arc-like pattern as the ionizing radiation encounters the dense gas, forming a blister-shaped morphology. We found three distinct young stellar groups, all coincident with relatively dense parts of the cloud complex, signifying ongoing star formation. Moreover, the cloud filament (excitation temperature $\sim$ 10 K) traced by the CO isotopologues and extending nearly $\sim$ 80 pc is devoid of ionized gas except at the dense cores (excitation temperature $\sim$ 28–32 K) wherein significant ionized emission excited by OB stars (dynamical age $\sim$ 0.18–1.0 Myr) pertains. The radial velocity is dynamic (median ~ -3.65 km s^{-1}) along the main filament, increasing from Galactic east to west, features mass flow to form the massive stars/clusters at the central hubs.

47. Making BEASTies: dynamical formation of planetary systems around massive stars

Richard J. Parker, Emma C. Daffern-Powell ★ Exoplanets display incredible diversity, from planetary system architectures around Sun-like stars that are very different to our Solar System, to planets orbiting post-main sequence stars or stellar remnants. Recently the B-star Exoplanet Abundance STudy (BEAST) reported the discovery of at least two super-Jovian planets orbiting massive stars in the Sco Cen OB association. Whilst such massive stars do have Keplerian discs, it is hard to envisage gas giant planets being able to form in such hostile environments. We use N-body simulations of star-forming regions to show that these systems can instead form from the capture of a free-floating planet, or the direct theft of a planet from one star to another, more massive star. We find that this occurs on average once in the first 10Myr of an association's evolution, and that the semimajor axes of the hitherto confirmed BEAST planets (290 and 556au) are more consistent with capture than theft. Our results lend further credence to the notion that planets on more distant (>100au) orbits may not be orbiting their parent star.

48. Discovery of a brown dwarf with quasi-spherical mass-loss

Dary A. Ruíz-Rodríguez, Lucas A. Cieza, Simon Casassus, Victor Almendros-Abad, Paula Jofré, Koraljka Muzic, Karla Peña Ramirez, Grace Batalla-Falcon, Michael M. Dunham, Camilo González-Ruilova, Antonio Hales, Elizabeth Humphreys, Pedro H. Nogueira, Claudia Paladini, John Tobin, Jonathan P. Williams, Alice Zurlo ★ We report the serendipitous discovery of an elliptical shell of CO associated with the faint stellar object SSTc2d J163134.1-24006 as part of the "Ophiuchus Disk Survey Employing ALMA" (ODISEA), a project aiming to study the entire population of protoplanetary disks in the Ophiuchus Molecular Cloud from 230 GHz continuum emission and ^{12}CO (J=2-1), ^{13}CO (J=2-1) and C^{18}CO (J=2-1) lines readable in Band-6. Remarkably, we detect a bright ^{12}CO elliptical shape emission of $\sim 3'' \times 4''$ towards SSTc2d J163134.1-24006 without a 230 GHz continuum detection. Based on the observed near-IR spectrum taken with the Very Large Telescope (KMOS), the brightness of the source, its 3-dimensional motion, and Galactic dynamic arguments, we conclude that the source is not a giant star in the distant background (>5 - 10 kpc) and is most likely to be a young brown dwarf in the Ophiuchus cloud, at a distance of just $\sim$139 pc. This is the first report of quasi-spherical mass loss in a young brown dwarf. We suggest that the observed shell could be associated with a thermal pulse produced by the fusion of deuterium, which is not yet well understood, but for a sub-stellar object is expected to occur during a short period of time at an age of a few Myr, in agreement with the ages of the objects in the region. Other more exotic scenarios, such as a merger with planetary companions, cannot be ruled out from the current observations.

49. Dynamics of young stellar clusters as planet forming environments

Megan Reiter, Richalsrd J. Parker ★ Most stars and thus most planetary systems do not form in isolation. The larger star-forming environment affects protoplanetary disks in multiple ways: gravitational interactions with other stars truncate disks and alter the architectures of exoplanet systems; external irradiation from nearby high-mass stars truncates disks and shortens their lifetimes; and remaining gas and dust in the environment affects dynamical evolution (if removed by feedback processes) and provides some shielding for disks from external irradiation. The dynamical evolution of the region regulates when and how long various feedback mechanisms impact protoplanetary disks. Density is a key parameter that regulates the intensity and duration of UV irradiation and the frequency of dynamical encounters. The evolution of larger star-forming complexes may also play an important role by mixing populations. Observations suggest that clusters are not a single-age population but multiple populations with small age differences which may be key to resolving several timescale issues (i.e., proplyd lifetimes, enrichment). In this review, we consider stellar clusters as the ecosystems in which most stars and therefore most planets form. We review recent observational and theoretical results and highlight upcoming contributions from facilities expected to begin observations in the next five years. Looking further ahead, we argue that the next frontier is large-scale surveys of low-mass stars in more distant high-mass star-forming regions. The future of ecosystem studies is bright as faint low-mass stars in more distant high-mass star-forming regions will be routinely observable in the era of Extremely Large Telescopes (ELTs).

50. Inside-Out Planet Formation. VII. Astrochemical Models of Protoplanetary Disks and Implications for Planetary Compositions

Arturo Cevallos Soto, Jonathan C. Tan, Xiao Hu, Chia-Jung Hsu, Catherine Walsh ★ Inside-Out Planet Formation (IOPF) proposes that the abundant systems of close-in Super-Earths and Mini-Neptunes form in situ at the pressure maximum associated with the Dead Zone Inner Boundary (DZIB). We present a model of physical and chemical evolution of protoplanetary disk midplanes that follows gas advection, radial drift of pebbles and gas-grain chemistry to predict abundances from 300 au down to the DZIB near 0.2 au. We consider typical disk properties relevant for IOPF, i.e., accretion rates 1E-9 < dM/dt / (Msun/yr) < 1E-8 and viscosity parameter alpha = 1E-4, and evolve for fiducial duration of t = 1E5 years. For outer, cool disk regions, we find that C and up to 90% of O nuclei start locked in CO and O2 ice, which keeps abundances of CO2 and H2O one order of magnitude lower. Radial drift of icy pebbles is influential, with gas-phase abundances of volatiles enhanced up to two orders of magnitude at ice-lines, while the outer disk becomes depleted of dust. Disks with decreasing accretion rates gradually cool, which draws in icelines closer to the star. At < 1 au, advective models yield water-rich gas with C/O ratios < 0.1, which may be inherited by atmospheres of planets forming here via IOPF. For planetary interiors built by pebble accretion, IOPF predicts volatile-poor compositions. However, advectively-enhanced volatile mass fractions of 10% can occur at the water ice line.

51. Molecular Fraction in the Galactic Center: The Central Molecular and HI Zones

Yoshiaki Sofue ★ By mapping the molecular fraction of the Galactic Center (GC), we quantitatively address the question of how much molecular and central the CMZ (Central Molecular Zone) is. For this purpose we analyze the CO and HI-line archival data, and determine the column- (surface-) and volume-molecular fractions, $f^{\Sigma}_{\rm mol}$ and $f^{\rho}_{\rm mol}$, which are the ratio of column-mass density of H_2 projected on the sky to that of total gas (H_2 + HI) from the line intensities, and the ratio of volume-mass densities of H_2 to total gas from the brightness temperature, respectively. It is shown that $f^{\Sigma}_{\rm mol}$ is as high as $\sim 0.9-0.95$ in the CMZ, and $f^{\rho}_{\rm mol}$ is $0.93-0.98$ in the GC Arms I and II attaining the highest value of ~ 0.98 toward Sgr B2. The expanding molecular ring (EMR, or the parallelogram) has a slightly smaller $f^{\Sigma}_{\rm mol}$ as $\sim 0.9-0.93$. We define the CMZ as the region with $f^{\Sigma}_{\rm mol} \geq 0.8-0.9$ between the shoulders of plateau-like distribution of H_2 column density from $l = -1^\circ.1$ to $+1^\circ.8$ having Gaussian vertical distribution with a half thickness of $\pm 0^\circ.2$. The CMZ is embedded in the Central HI Zone (CHZ), which is defined as an HI disc between $l \sim -2^\circ$ and $+2^\circ.5$, $b = -0^\circ.5$ and $+0^\circ.5$. Based on the analysis, we discuss the origin of CMZ and interstellar physics such as the volume filling factors of molecular and HI gases inferred from the difference between $f^{\Sigma}_{\rm mol}$ and $f^{\rho}_{\rm mol}$.

52. StraKLIP: A novel pipeline for detection and characterization of close-in faint companions through Karhunen-Loêve Image Processing algorithm

Giovanni M. Strampelli, Laurent Pueyo, Jonathan Aguilar, Antonio Aparicio, Gaspard Duchêne, Massimo Robberto ★ We present a new pipeline developed to detect and characterize faint astronomical companions at small angular separation from the host star using sets of wide-field imaging observations not specifically designed for High Contrast Imaging analysis. The core of the pipeline relies on Karhunen-Loêve truncated transformation of the reference PSF library to perform

PSF subtraction and identify candidates. Tests of reliability of detections and characterization of companions are made through simulation of binaries and generation of Receiver Operating Characteristic curves for false positive/true positive analysis. The algorithm has been successfully tested on large HST/ACS and WFC3 datasets acquired for two HST Treasury Programs on the Orion Nebula Cluster. Based on these extensive numerical experiments we find that, despite being based on methods designed for observations of single star at a time, our pipeline performs very well on mosaic space based data. In fact, we are able to detect brown dwarf-mass companions almost down to the planetary mass limit. The pipeline is able to reliably detect signals at separations as close as $\gtrsim 0.1$" with a completeness of $\gtrsim 10\%$, or ~ 0.2" with a completeness of $\sim 30\%$. This approach can potentially be applied to a wide variety of space based imaging surveys, starting with data in the existing HST archive, near-future JWST mosaics, and future wide-field Roman images.

53. Rogue planets and brown dwarfs: Predicting the populations of free-floating planetary mass objects observable with JWST

Aleks Scholz, Koraljka Muzic, Ray Jayawardhana, Lyra Quinlan, James Wurster ★ Free-floating (or rogue) planets are planets that are liberated (or ejected) from their host systems. Although simulations predict their existence in substantial numbers, direct observational evidence for free-floating planets with masses below 5 MJup is still lacking. Several cycle-1 observing programs with JWST aim to hunt for them in four different star-forming clusters. These surveys are designed to be sensitive to masses of 1-15 MJup (assuming a hot-start formation), which corresponds to spectral types of early L to late T for the ages of these clusters. If the existing simulations are not wide off the mark, we show here that the planned programs are likely to find up to 10-20 giant rogue planets in moderate density clusters like NGC1333 or IC348, and several dozen to 100 in high-density regions like NGC2024 and the Orion Nebula Cluster. These numbers correspond to 1-5% of the total cluster population; they could be substantially higher if stars form multiple giant planets at birth. In contrast, the number of free-floating brown dwarfs, formed from core collapse ("like stars") is expected to be significantly lower, only about 0.25number of stars, or 1-7 for the clusters considered here. Below 10 MJup that number drops further by an order of magnitude. We also show that the planned surveys are not at risk of being significantly contaminated by field brown dwarfs in the foreground or background, after spectroscopic confirmation. Taken together, our results imply that if a population of L and T dwarfs were to be found in these JWST surveys, it is expected to be predominantly made up of rogue planets.

54. ATOMS: ALMA Three-millimeter Observations of Massive Star-forming regions – XII: Fragmentation and multi-scale gas kinematics in protoclusters G12.42+0.50 and G19.88-0.53

Anindya Saha, Anandmayee Tej, Hong-Li Liu, Tie Liu, Namitha Issac, Chang Won Lee, Guido Garay, Paul F. Goldsmith, Mika Juvela, Sheng-Li Qin, Amelia Stutz, Shanghuo Li, Ke Wang, Tapas Baug, Leonardo Bronfman, Feng-Wei Xu, Yong Zhang, Chakali Eswaraiah ★ We present new continuum and molecular line data from the ALMA Three-millimeter Observations of Massive Star-forming regions (ATOMS) survey for the two protoclusters, G12.42+0.50 and G19.88-0.53. The 3 mm continuum maps reveal seven cores in each of the two globally contracting protoclusters. These cores satisfy the radius-mass relation and the surface mass density criteria for high-mass star formation. Similar to their natal clumps, the virial analysis of the cores suggests that they are undergoing gravitational collapse ($\alpha_{\rm vir} << 2$). The clump to core scale fragmentation is investigated and the derived core masses and separations are found to be consistent with thermal Jeans fragmentation. We detect large-scale filamentary structures with velocity gradients and multiple outflows in both regions. Dendrogram analysis of the $H^{13}CO^+$ map identifies several branch and leaf structures with sizes ~ 0.1 and 0.03 pc, respectively. The supersonic gas motion displayed by the branch structures is in agreement with the Larson power-law indicating that the gas kinematics at this spatial scale is driven by turbulence. The transition to transonic/subsonic gas motion is seen to occur at spatial scales of $\sim$0.1 pc indicating the dissipation of turbulence. In agreement with this, the leaf structures reveal gas motions that deviate from the slope of Larson's law. From the large-scale converging filaments to the collapsing cores, the gas dynamics in G12.42+0.50 and G19.88-0.53 show scale-dependent dominance of turbulence and gravity and the combination of these two driving mechanisms needs to be invoked to explain massive star formation in the protoclusters.

55. Core orientations and magnetic fields in isolated molecular clouds

Ekta Sharma, Maheswar Gopinathan, Archana Soam, Chang Won Lee, T. R. Seshadri ★ Molecular clouds are sites of star formation. Magnetic fields are believed to play an important role in their dynamics and shaping morphology. We aim to study any possible correlation that might exist between the magnetic fields orientation inside the clouds and the magnetic fields at envelope scales and their connection with respect to the observed morphology of the selected clouds. We examine the magnetic field orientation towards the clouds L1512, L1523, L1333, L1521E, L1544, L1517, L1780, and L183 using optical and *Planck* polarization observations. We also found the correlation between the ambient magnetic field and core orientations derived using *Astrodendrogram* on the *Herschel* 250 μm data. We find that the magnetic fields derived from optical and *Planck* agree with each other. The derived magnetic fields are aligned along the observed emission of each cloud as seen in *Herschel* 250 μm data. We also find that the relative orientation between the cores and the magnetic fields is random. This lack of correlation may arise due to the fact that the core orientation could also be influenced by the different magnetization within individual clouds at higher densities or the feedback effects which may vary from cloud to cloud. The estimated magnetic field strength and the mass-to-flux ratio suggest that all the clouds are in a magnetically critical state except L1333, L1521E, and L183 where the cloud envelope could be strongly supported by the magnetic field lines.

56. Bird's eye view of molecular clouds in the Milky Way: II. Cloud kinematics from sub-pc to kpc scales

Andri Spilker, Jouni Kainulainen, Jan Orkisz ★ The kinematics of molecular gas are crucial for setting the stage for star formation. One key question related to the kinematic properties of gas is how they depend on the spatial scale. We aim to describe the CO spectra, velocity dispersions, and especially the linewidth-size relation, of molecular gas from cloud (parsec-) scales to kiloparsec scales in a complete region within the Milky Way disk. We utilise the census of molecular clouds within 2 kpc from our earlier work, together with CO emission data for them from the literature. We study the kinematics and the Larson's relations for the sample of individual clouds. We also mimic a face-on view of the Milky Way and analyse the kinematics of the clouds within apertures of 0.25-2 kpc in size. In this way, we describe the scale-dependency of the CO gas kinematics and Larson's relations. We describe the spectra of CO gas at cloud scales and in apertures between 0.25-2 kpc in our survey area. The spectra within the apertures are relatively symmetric but show non-Gaussian high-velocity wings. At cloud-scales, our sample shows a linewidth-size relation $\sigma_v = 1.5 \times R^{0.3\pm0.1}$ with a large scatter. The mass-size relation in the sample of clouds is $M_{CO} = 794 \times R^{1.5\pm0.5}$. The relations are also present for the apertures at kpc-scales. A suggestive dependency on galactic environment is seen, with apertures closer to the Galactic centre and the Sagittarius spiral arm having slightly higher velocity dispersions. We explore the possible effect of a diffuse component in the survey area, and find that such a component would widen the CO spectra and could flatten the linewidth-size relation. Understanding the nature of the possible diffuse CO component and its effects on observations is crucial for connecting Galactic and extragalactic data.

57. The imprint of star formation on stellar pulsations

Thomas Steindl, Konstanze Zwintz, Eduard Vorobyov ★ In the earliest phases of their evolution, stars gain mass through the acquisition of matter from their birth clouds. The widely accepted classical concept of early stellar evolution neglects the details of this accretion phase and assumes the formation of stars with large initial radii that contract gravitationally. In this picture, the common idea is that once the stars begin their fusion processes, they have forgotten their past. By analysing stellar oscillations in recently born stars, we show that the accretion history leaves a potentially detectable imprint on the stars' interior structures. Currently available data from space would allow discriminating between these more realistic accretion scenarios and the classical early stellar evolution models. This opens a window to investigate the interior structures of young pulsating stars that will also be of relevance for related fields, such as stellar oscillations in general and exoplanet studies.

58. Disk Evolution Study Through Imaging of Nearby Young Stars (DESTINYS): Scattered light detection of a possible disk wind in RY Tau

P. -G. Valegård, C. Ginski, C. Dominik, J. Bae, M. Benisty, T. Birnstiel, S. Facchini, A. Garufi, M. Hogerheijde, R. G. van Holstein, M. Langlois, C. F. Manara, P. Pinilla, Ch. Rab, Á. Ribas, L. B. F. M. Waters, J. Williams ★ Disk winds are an important mechanism for accretion and disk evolution around young stars. The accreting intermediate-mass T-Tauri star RY Tau has an active jet and a previously known disk wind. Archival optical and new near-infrared observations of the RY Tau system show two horn-like components stretching out as a cone from RY Tau. Scattered light from the disk around RY Tau is visible in near-infrared but not seen at optical wavelengths. In the near-infrared, dark wedges that separates the horns from the disk, indicating we may see the scattered light from a disk wind. We use archived ALMA and SPHERE/ZIMPOL I-band observations combined with newly acquired SPEHRE/IRDIS H-band observations and available literature to build a simple geometric model of the RY Tau disk and disk wind. We use Monte Carlo radiative transfer modelling *MCMax3D* to create comparable synthetic observations that test the effect of a dusty wind on the optical effect in the observations. We constrain the grain size and dust mass needed in the disk wind to reproduce the effect from the observations. A model geometrically reminiscent of a dusty disk wind with small micron to sub-micron size grains elevated above the disk can reproduce the optical effect seen in the observations. The mass in the obscuring component of the wind has been constrained to $1 \times 10^{-9} M_\odot \leq M \leq 5 \times 10^{-8} M_\odot$ which corresponds to a lower limit mass loss rate in the wind of about $\sim 1 \times 10^{-8} M_\odot \mathrm{yr}^{-1}$. While an illuminate dust cavity cannot be ruled out without measurements of the gas velocity, we argue that a magnetically launched disk wind is the most likely scenario.

59. Physical properties of accretion shocks toward the Class I protostellar system Oph-IRS 44

E. Artur de la Villarmois, V. V. Guzmán, J. K. Jørgensen, L. E. Kristensen, E. A. Bergin, D. Harsono, N. Sakai, E. F. van Dishoeck, S. Yamamoto ★ (Abridged) Physical processes such as accretion shocks are thought to be common in the protostellar phase, where the envelope component is still present, and they can release molecules from the dust to the gas phase, altering the original chemical composition of the disk. Consequently, the study of accretion shocks is essential for a better understanding of the physical processes at disk scales and their chemical output. The purpose of this work is to assess the characteristics of accretion shocks traced by sulfur-related species. We present ALMA high angular resolution observations (0.1") of the Class I protostar Oph-IRS 44. The continuum emission at 0.87 mm is observed, together with sulfur-related species such as SO, SO_2, and $^{34}SO_2$. Six lines of SO_2, two lines of $^{34}SO_2$, and one line of SO are detected toward IRS 44. The emission of all the detected lines peaks at 0.1" (14 au) from the continuum peak and we find infalling-rotating motions inside 30 au. However, only redshifted emission is seen between 50 and 30 au. Colder and more quiescent material is seen toward an offset region located at a distance of 400 au from the protostar, and we do not find evidence of a Keplerian profile in these data. Accretion shocks are the most plausible explanation for the high temperatures, high densities, and velocities found for the SO_2 emission. When material enters the disk–envelope system, it generates accretion shocks that increase the dust temperature and desorb SO_2 molecules from dust grains. High-energy SO_2 transitions (200 K) seem to be the best tracers of accretion shocks that can be followed up by future higher angular resolution ALMA observations and compared to other species to assess their importance in releasing molecules from the dust to the gas phase.

60. Multi-wavelength Observations of MWC 297: Constraints on Disk Inclination and Mass Outflow

William D. Vacca, Göran Sandell ★ MWC 297 is a young, early-type star driving an ionized outflow and surrounded by warm, entrained dust. Previous analyses of near- and mid-IR interferometric images suggest that the emission at these wavelengths arises from a compact accretion disk with a moderate ($i < 40$ degrees) inclination. We have obtained 5-40 micron images of MWC 297 with FORCAST on SOFIA, as well as near-infrared spectra acquired with SpeX on the IRTF and radio data obtained with the VLA and BIMA, and supplemented these with archival data from Herschel/PACS and SPIRE. The FORCAST images, combined with the VLA data, indicate that the outflow lobes are aligned nearly north-south and are well separated. Simple geometrical modeling of the FORCAST images suggests that the disk driving the outflow has an inclination of 55 ± 5 degrees, in disagreement with the results of the interferometric analyses. Analysis of the SpeX data, with a wind model, suggests the the mass loss rate is on the order of $6.0\pm^{3.7}_{1.7}\times10^{-7} M_\odot$ yr^{-1} and the extinction to the source is $A_V \sim 8.1\pm^{2.5}_{1.5}$ mag. We have combined our data with values from the literature to generate the spectral energy distribution of the source from 0.35 μm to 6 cm and estimate the total luminosity. We find the total luminosity to be about 7900 $L_\odot$, if we include emission from an extended region around the star, only slightly below that expected for a B1.5V star. The reddening must be produced by dust along the line of sight, but distant from the star.

61. Confirmation of the outflow in L1451-mm: SiO line and CH_3OH maser detections

V. Wakelam, A. Coutens, P. Gratier, T. H G Vidal, N. Vaytet ★ The observational counterparts of theoretically predicted first hydrostatic cores (FHSC) have been searched for in the interstellar medium for nearly two decades now. Distinguishing them from other types of more evolved but still embedded objects remains a challenge because these objects have a short lifetime, are small, and embedded in a dense cocoon. One possible lead to finding them is the characterization of the outflows that are launched by these objects. We observed the L1451-mm FHSC candidate with the NOEMA interferometer in order to study the emission of several molecules. A nonlocal thermodynamic equilibrium analysis of the CH_3OH detected lines was performed to retrieve the physical conditions of the emitting region around the central source, together with the CH_3OH, SiO, CS, and H_2CO column densities. Of the targeted molecules, we detected lines of c-C_3H_2, CH_3OH, CS, $C^{34}S$, SO, DCN, DCO^+, H_2CO, HC_3N, HDCO, and SiO. One of the methanol lines appears to be a maser line. The detection of this class I maser and the SiO line in L1451-mm support the presence of a low-velocity and compact outflow. The excitation conditions of the thermal lines of methanol are also compatible with shocks (H_2 density of $\sim 3 \times 10^6$ cm^{-3} and a temperature higher than 40 K). Although these low-velocity outflows are theoretically predicted by some models of FHSC, these models also predict the shock temperature to be below 20 K, that is, not evaporating methanol. In addition, the predicted velocities would not erode the grains and release silicon in the gas phase. We therefore conclude that these new observations favor the hypothesis that L1451-mm would be at a very early protostellar stage, launching an outflow nearly on the plane of the sky with a higher velocity than is observed.

62. ALMA uncovers highly filamentary structure towards the Sgr E region

J. Wallace, C. Battersby, E. A. C. Mills, J. D. Henshaw, M. C. Sormani, A. Ginsburg, A. T. Barnes, H. P. Hatchfield, S. C. O. Glover, L. D. Anderson ★ We report on the discovery of linear filaments observed in CO(1-0) emission for a $\sim 2'$ field of view toward the Sgr E star forming region centered at (l,b)=(358.720°, 0.011°). The Sgr E region is thought to be at the turbulent intersection of the "far dust lane" associated with the Galactic bar and the Central Molecular Zone (CMZ). This region is subject to strong accelerations which are generally thought to inhibit star formation, yet Sgr E contains a large number of HII regions. We present ^{12}CO(1-0), ^{13}CO(1-0), and C^{18}O(1-0) spectral line observations from ALMA and provide measurements of the physical and kinematic properties for two of the brightest filaments. These filaments have widths (FWHM) of ~ 0.1 pc and are oriented nearly parallel to the Galactic plane, with angles from the Galactic plane of $\sim 2°$. The filaments are elongated, with lower limit aspect ratios of $\sim$5:1. For both filaments we detect two distinct velocity components that are separated by about 15 km s^{-1}. In the C^{18}O spectral line data with $\sim$0.09 pc spatial resolution, we find that these velocity components have relatively narrow ($\sim$1-2 km s^{-1}) FWHM linewidths when compared to other sources towards the Galactic center. The properties of these filaments suggest that the gas in the Sgr E complex is being "stretched" as it is rapidly accelerated by the gravitational field of the Galactic bar while falling towards the CMZ, a result that could provide insight into the extreme environment surrounding this region and the large-scale processes which fuel this environment.

63. Discovery of Line Pressure Broadening and Direct Constraint on Gas Surface Density in a Protoplanetary Disk

Tomohiro C. Yoshida, Hideko Nomura, Takashi Tsukagoshi, Kenji Furuya, Takahiro Ueda ★ The gas surface density profile of protoplanetary disks is one of the most fundamental physical properties to understand planet formation. However, it is challenging to determine the surface density profile observationally, because the H_2 emission cannot be observed in low-temperature regions. We analyzed the Atacama Large Millimeter/submillimeter Array (ALMA) archival data of the CO line toward the protoplanetary disk around TW Hya and discovered extremely broad line wings due to the pressure broadening. In conjunction with a previously reported optically thin CO isotopologue line, the pressure broadened line wings enabled us to directly determine the midplane gas density for the first time. The gas surface density at ~ 5 au from the central star reaches $\sim 10^3$ g cm^{-2}, which suggests that the inner region of the disk has enough mass to form a Jupiter-mass planet. Additionally, the gas surface density drops at the inner cavity by ~ 2 orders of magnitude compared to outside the cavity. We also found a low CO abundance of $\sim 10^{-6}$ with respect to H_2, even inside the CO snowline, which suggests conversion of CO to less volatile species. Combining our results with previous studies, the gas surface density jumps at $r \sim 20$ au, suggesting that the inner region ($3 < r < 20$ au) might be the magnetorotational instability dead zone. This study sheds light on direct gas-surface-density constraint without assuming the CO/H_2 ratio using ALMA.

64. Directly Detecting the Envelopes of Low-mass Planets Embedded In Protoplanetary Discs and The Case For TW Hydrae

Zhaohuan Zhu, Avery Bailey, Enrique Macías, Takayuki Muto, Sean M. Andrews ★ Despite many methods developed to find young massive planets in protoplanetary discs, it is challenging to directly detect low-mass planets that are embedded in discs. On the other hand, the core-accretion theory suggests that there could be a large population of embedded low-mass young planets at the Kelvin-Helmholtz (KH) contraction phase. We adopt both 1-D models and 3-D simulations to calculate the envelopes around low-mass cores (several to tens of $M_\oplus$) with different luminosities, and derive their thermal fluxes at radio wavelengths. We find that, when the background disc is optically thin at radio wavelengths, radio observations can see through the disc and probe the denser envelope within the planet's Hill sphere. When the optically thin disc is observed with the resolution reaching one disc scale height, the radio thermal flux from the planetary envelope around a 10 $M_\oplus$ core is more than 10% higher than the flux from the background disc. The emitting region can be extended and elongated. Finally, our model suggests that the au-scale clump at 52 au in the TW Hydrae disc revealed by ALMA is consistent with the envelope of an embedded 10-20 $M_\oplus$ planet, which can explain the detected flux, the spectral index dip, and the tentative spirals. The observation is also consistent with the planet undergoing pebble accretion. Future ALMA and ngVLA observations may directly reveal more such low-mass planets, enabling us to study core growth and even reconstruct the planet formation history using the embedded "protoplanet" population.

65. RVSPY – Radial Velocity Survey for Planets around Young Stars. Target characterization and high-cadence survey

O. Zakhozhay, R. Launhardt, A. Mueller, S. Brems, P. Eigenthaler, M. Gennaro, A. Hempel, M. Hempel, Th. Henning, G. Kennedy, S. Kim, M. Kuerster, R. Lachaume, Y. Manerikar, J. Patel, A. Pavlov, S. Reffert, T. Trifonov ★ We introduce our Radial Velocity Survey for Planets around Young stars (RVSPY), characterise our target stars, and search for substellar companions at orbital separations smaller than a few au from the host star. We use the FEROS spectrograph to obtain high signal-to-noise spectra and time series of precise radial velocities (RVs) of 111 stars most of which are surrounded by debris discs. Our target stars have spectral types between early F and late K, a median age of 400 Myr, and a median distance of 45 pc. We determine for all target stars their basic stellar parameters and present the results of the high-cadence RV survey and activity characterization. We achieve a median single-measurement RV precision of 6 m/s and derive the short-term intrinsic RV scatter of our targets (median 22 m/s), which is mostly caused by stellar activity and decays with age from $>$100 m/s at $<$20 Myr to $<$20 m/s at $>$500 Myr. We discover six previously unknown close companions with orbital periods between 10 and 100 days, three of which are low-mass stars, and three are in the brown dwarf mass regime. We detect no hot companion with an orbital period $<$10 days down to a median mass limit of 1 M_{Jup} for stars younger than 500 Myr, which is still compatible with the established occurrence rate of such companions around main-sequence stars. We find significant RV periodicities between 1.3 and 4.5 days for 14 stars, which are, however, all caused by rotational modulation due to starspots. We also analyse the TESS photometric time series data and find significant periodicities for most of the stars. For 11 stars, the photometric periods are also clearly detected in the RV data. We also derive stellar rotation periods ranging from 1 to 10 days for 91 stars, mostly from TESS data. From the intrinsic activity-related short-term RV jitter, we derive the expected mass-detection thresholds for longer-period companions.